DSPACE

https://dspace.org/

The attenuation of the main zone at the Phosiri Dome, Bushveld Complex

Martin, Lucienne E

2011-05-16
http://hdl.handle.net/10539/9776

Downloaded from a DSpace repository. https://dspace.org/

adjacent samples. The sample at -19m, however, indicates an obvious break in the R_O, from the sequence of samples immediately below this depth, although it is in keeping with the values defined by Kruger (1994) for the Differentiation Stage. For these five samples, rubidium is high and contained within potassium feldspar, it is believed to have been introduced by the hydrothermal fluids percolating through fault zones.

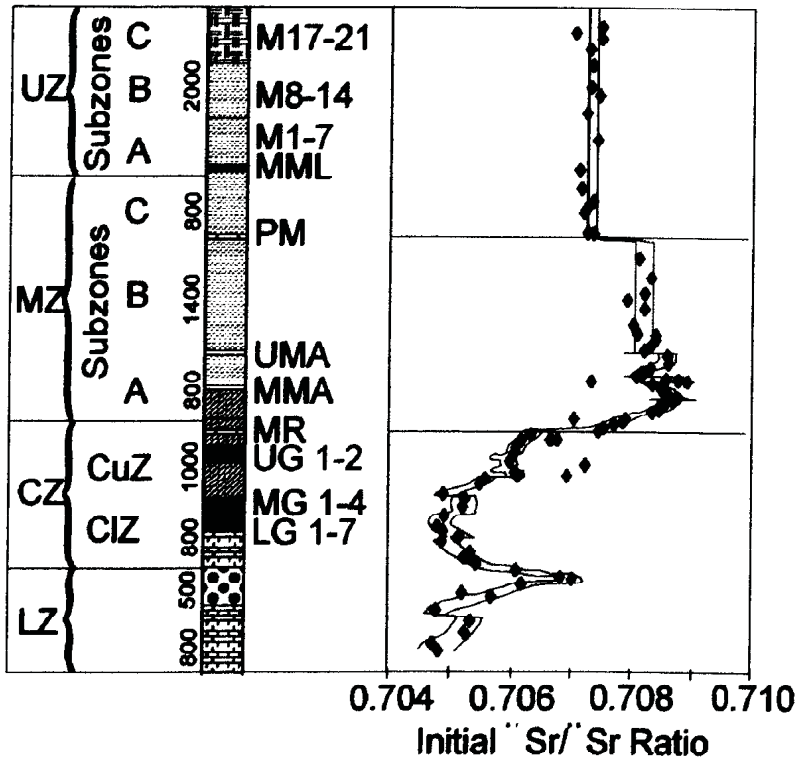


Figure 8.C Complete initial profile of the initial ratio through the Bushveld Complex in the western limb, after Kruger (1994), with data acquired from Teigler (1990), Eales *et al.* (1990), Mitchell (1986), Cawthorn *et al.* (1991) and Kruger *et al.* (1987).

9: DISCUSSION AND CONCLUSIONS

From a review of available sources, it was possible to construct a typical sequence for the Rustenburg Layered Suite of the Bushveld Complex. This sequence contained sufficient data to provide a model to compare with the results of petrographic, mineral, whole rock geochemistry, and strontium isotope analyses. These analyses, described in Chapters 4 to 8, all indicate that the sequence found in D1 and D2 is very much attenuated. Potential mechanisms for this attenuation are discussed first, followed by a review of the key findings for each zone. These findings are then compared, by zone, with the attenuation models to identify which mechanisms may potentially have caused the attenuation. The results of this analysis are used to develop a possible schematic cross-section of the sequence between D1 and D2 boreholes. Finally, suggestions for further work are proposed.

9.1: Models for the Attenuation at the Phosiri Dome

There are four possible explanations for the type of attenuation seen in the sequence of the Rustenburg Layered Suite. Each of these models may have occurred alone, or in combination, throughout the history of emplacement and tectonism:

- Lateral variation in the extent of magmatic influx.
- Thinning of the mafic sequence towards the diapiric structure.
- Faulting out of the mafic sequence.
- Magmatic influxes, although sequentially similar to the main body of the complex, may have been subjected to different magma mixing and differentiation processes.

9.1.1: Lateral Variation in the Extent of Magmatic Influx

Individual magmatic influxes may have originated from separate sources, thus the volume and viscosity of each influx would have varied and, consequently, the extent to which they travelled would also have differed. In addition, early influxes would have been channelled, by pre-existing sedimentary highs in the region, to form finger-like bodies on the lower ground (Uken and Watkeys, 1997). Hence, the depth of deposition of a distinct layer at a specific point would have depended upon previous depositions, i.e. it would have been thinner up-slope.

9.1.2: Thinning of the Mafic Sequence Units in the Vicinity of the Diapiric Structure

Uken and Watkeys (1997) also suggested that the pre-existing highs would have become the loci for subsequent floor-rock diapirism, which was initiated with the onset of further magmatic influxes. As the domes developed, the upward movement would have led to the viscous dragging of partially crystallised mafic units, causing the individual units to stretch and, consequently to thin. This process may explain the presence of chromitite and pyroxenite pods in the gullies, on the flanks of the Phosiri Dome.

9.1.3: Faulting Out of Mafic Units

The presence of hydrothermal alteration in the borehole is indicative of fault activity. Brittle deformation of various units throughout the typical Rustenburg Layered Suite would suggest that the process of diapirism had continued well after the emplacement and consolidation of the mafic sequence. The upward movement of the dome structure would have caused the onlapping lithologies to detach along planes of weakness. Where these planes of weakness occurred along either contacts between zones and subzones or along fault planes within the zones/subzones, detachment would have resulted in the absence of portions of the units, as is evident today. It is possible, therefore, that faulted out units, as a result of normal faulting, may be present down slope.

9.1.4: Magmatic Influxes Subjected to Different Magma Mixing and Differentiation Processes.

The crystallisation processes in different parts of the complex may undergo differentiation at different rates. This means that new material being introduced has the potential to mix with remaining magmatic material and therefore result in a different composition to that seen elsewhere in the complex. Also, a slower rate of differentiation would result in a continuous trend, with expected changes in mineralogy, indicating breaks in the sequence, essentially being disguised.

9.2: Critical Zone

The Critical Zone is only represented within D1, therefore all conclusions in this section refer to this borehole alone.

The lithology of the CIZ, in the borehole, is primarily composed of feldspathic pyroxenites with chromitites, but, significantly, there is no evidence of olivine. Five chromitites in the lower part of the succession, do appear to be part of the Lower Group (LG) chromitites, although no attempt was made

to compare layer with layer. However, located near the top of the ClZ, a second sequence of seven partings, thought to be chromitites of the Middle Group (MG), were matched to the MG1 and MG2. Importantly, although much of the sequence seems to be present, it is much thinner than the 800m thickness expected for this zone. Thinning in this zone is not unusual for the Bushveld Complex, as early deposition varied considerably across the complex. However, thinning could indicate the pre-existence of a structural high that restricted deposition. It could also point to the layer being faulted out through diapiric uplift. Furthermore, the lack of olivine suggests that the lower harzburgite units are missing. Faulting and fracturing, with subsequent late-stage alteration mineral assemblages, indicate that ductile and brittle deformation has occurred. The ductile deformation either occurred prior to the consolidation of the rocks or in high temperature regimes, whilst fracturing and alteration occurred along planes of weakness. Consequently, whole units and parts of particular lithologies, within the ClZ, have been removed, although how many or what fraction, cannot be determined.

The limits of the CuZ can be clearly observed in D1, with the onset of cumulus plagioclase in a norite at the base, and the Giant Mottled Anorthosite at the top of the zone. However, notable layers in the typical sequence are absent, including the MG3, MG4, UG1, UG2 and UG3 chromitites. Conversely, strontium analyses confirm the existence of the typical sequence that would be expected between the UG2 and the Merensky Reef. All of the analyses carried out confirm that the Merensky and Bastard Cyclic units would appear to be fully represented at the top of the sequence.

Although the typical sequence for the CuZ amounts to over 800m in thickness, the thickness of the interval between the UG2 and the top of the CuZ is variable. It is therefore possible that the entire CuZ, represented within 188m thickness in D1, may be comparable to this section between the UG2 and the top of the CuZ. Based on this last statement, it can be said that much of the typical sequence below, and including the UG2, is missing. As the sequence was probably deposited during diapirism, and there is no evidence of fracturing at the base of the subzone, it is more likely that the attenuation was a result of lateral variation, due to the restricted extent of magma influx on the flanks of the Phosiri Dome. Finally, although the mineral analyses were limited, the concentration trends are generally uniform. This may indicate that neither faulting nor lateral variation are apparent. However, lateral variation may not be obvious if the rate of change of mineral composition is extremely slow, as a function of height through the zone.

Although the strontium isotope analysis of samples, taken from the Merensky and Bastard Cyclic Units, agreed with other analyses, higher initial ratios were obtained for the Bastard Reef than obtained by other workers in both the eastern and western limbs. A break, marking the final stages of the Merensky event is not evident at the base of the Bastard Reef in D1. However, the initial ratios clearly indicate an inflection within the Merensky Cyclic Unit. The XRF data confirmed that the sequences above and below the Merensky Reef formed from two different magma influxes. In addition, electron microprobe analysis detected other breaks in the sequence, but these appeared to be

controlled by lithology. Therefore, it is possible that this inflection, coupled with the XRF analyses, indicates the position of the top of the Merensky Cyclic Unit.

Further alteration in the sequence is found as alteration of the minerals within the lithologies at the top of the zone. Hydrothermal fluids depositing alteration product minerals such as chlorite and epidote, indicate that there has been either faulting or shearing of units.

9.3: Main Zone

The limit of the base of the MZ is identified as the top of the GMA, and the upper constraint is the presence of magnetite, marking the start of the UZ. The MZ in D1 contains gabbronorites and anorthosites, with both the expected norites typically found at the base of Subzone A and Porphyritic Norite Marker absent, which would infer that only the upper portion of Subzone A is present. The strontium isotope initial ratios confirm that the gabbronoritic layers do indeed belong to Subzone A. Consequently, it is assumed that the lower portion of Subzone A is missing. Within D1, two anorthositic layers, may correspond to the MMA and UMA. These markers are only 69m apart, and when compared to the typical 565-900m interval, suggest that the upper portion of the subzone is also attenuated. It is therefore clear that D1 contains a partial, and much reduced lithological representation of Subzone A. The electron microprobe analyses results show a normal differentiation trend for the En content throughout the entire MZ in D1, which compares favourably with the Subzone A.

Petrographic observations show that there is no inverted pigeonite in the MZ, suggesting that the whole of Subzone B is missing; a conclusion corroborates by the strontium isotope analysis. The values derived from the lower part of the MZ in D1 could all come from Subzone A alone. The initial ratio calculated for the uppermost sample in the MZ, however, is the same as the typical values for above the Pyroxenite Marker. It is therefore concluded that Subzone B is absent.

It was found that the presence of intercalated pyroxenite, within a leucogabbronorite in D1, and a corresponding reversal in initial ratio, fixed the position the Pyroxenite Marker and, therefore, the boundary between Subzones A and C, approximately 20m below the top of the MZ. Because the initial ratio is not controlled by lithology, the boundary, which indicated a magmatic influx, will occur regardless of the thickness, or indeed, the absence of subzones. Thus, Subzone C is also present within D1, but only in a 19m thick sequence, compared with 660-690m of the typical. Below the position of the Pyroxenite Marker, a gabbronorite contains hydrothermal alteration products, similar to those found in lithologies encountered both above the marker and within Subzone A. There is little direct evidence for any normal faulting having been responsible for the absence of Subzone C. This

may suggest that the absent portions are as a result of the timing of crystallisation taking longer through the Main Zone.

Looking at the evidence presented for D2, no geochemical breaks are evident. Importantly, the reversal seen in initial ratio at the Pyroxenite Marker is absent, but the range of values obtained for the initial ratio corresponds to typical values for above the Pyroxenite Marker. This assessment is supported by the strontium concentrations in D2, which are comparable with those found directly above the Pyroxenite Marker in the typical sequence. This is significant in that the entire sequence in D2 would appear to lie stratigraphically above this marker. Along with corroborating data from the petrographic and geochemical evidence, it is determined that only Subzone C of the MZ is present. However, as this zone is devoid of prominent markers, the 152m Subzone C cannot be directly matched to any of the typically found units with any confidence. As for D1, it can be seen that this unit is severely attenuated, when compared with the typical sequence.

9.4: Upper Zone

The appearance of magnetite marks the position of the lower boundary of the UZ in both D1 and D2. The UZ in D1 is greater than 240m thick, and from petrographic evidence compares well with the typical Subzone A, although much attenuated. Magnetite layers in D2 also correspond with Subzone A magnetites, with two samples matching magnetite layers situated below the MML. The inferred position of the MML in D2, based on analyses of the magnetite layers, suggests that Subzone A is severely attenuated. There is no evidence of olivine in either D1 or D2, thus indicating that the residual units of both borecores come only from Subzone A. Interestingly, although Subzones B and C are not present within the boreholes, further analyses carried out on surface samples from the site show Subzone B characteristics. There is no evidence to suggest the presence of Subzone C.

9.5: Overview

In this structurally uplifted area, it is possible that the diapiric activity of the Phosiri Dome resulted in a much-attenuated sequence of the mafic lithologies of the Rustenburg Layered Suite. The two boreholes, used in this study, provided information that was useful in determining how the typical sequence might be affected by such events. A schematic cross section reconstruction of the units between D1 and D2, shown in Figure 9.A, illustrates that Subzone B of the MZ could, as a result of normal faulting, be present to the southwest of the Phosiri Dome. Evidence for faulting is not convincing for the absence of many of the other portions of the sequence, which may be absent as a result of slow crystallisation and limited lateral extent of the magmatic influx. The anomalously shallow depth at which the MZ/UZ boundary occurs in D2 is explained by the presence of another

upfold in the sequence. Other tectonically uplifted areas, within the Bushveld Complex, exhibit similar condensed sequences. At Malope Dome, situated southwest of the Phosiri Dome, the Upper Zone rests upon a very much-attenuated succession of MZ lithologies.

Although neither of the boreholes used in this study contain full successions, when compared with the normal stratigraphic sequence, they do overlap, with D2 lying mostly above D1. Together, they give a more comprehensive representation of what is typically expected. From the base of the sequence, the ClZ, CuZ and Subzone A of the MZ are represented by D1 with Subzone B missing altogether. Only 19m of Subzone C is present in D1, with a much larger component of the equivalent unit seen in D2. The UZ is present in both borecores, both of which contain Subzone A only.

The attenuated units have resulted in the mineable layer in D1, *i.e.* the Merensky Reef, being brought closer to the surface. This phenomenon, therefore, makes the Phosiri Dome a more attractive target area for exploration. However, only 2.2km away in a southwesterly direction, the lithologies in D2 create a different impression of the area altogether. With only Subzone C of the MZ present, and no indication of the Pyroxenite Marker, it is impossible to ascertain whether Subzones A or B of this zone are in fact present, and, consequently, at what depth the Merensky Reef would be located.

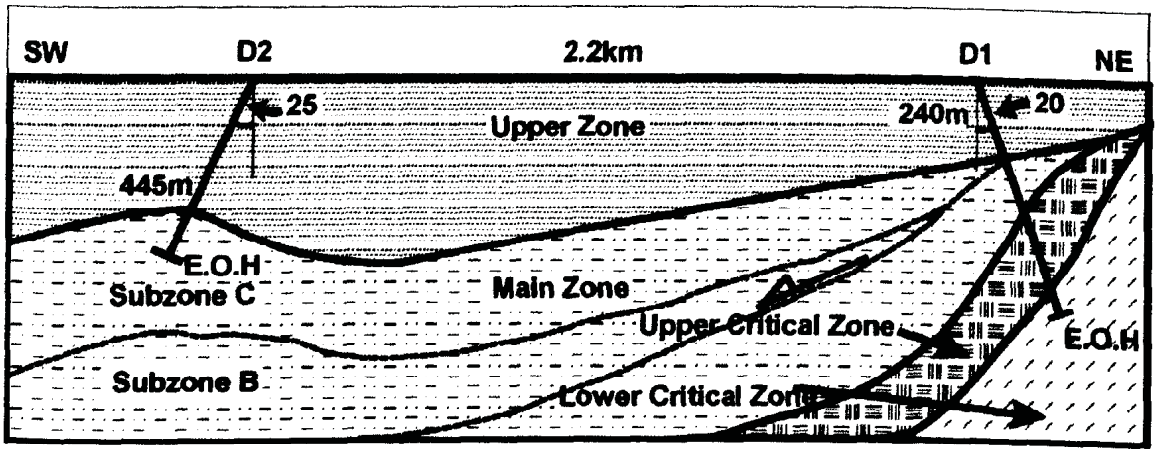


Figure 9.A Schematic representation of the cross section of the Bushveld Complex Units between D1 and D2. The boundaries between Subzones A, B and C of the Main Zone are inferred to pinch out towards the Phosiri Dome in the northeast, with the presence of Subzone B inferred to be to the SW as a result of fault activity.

9.6: Further Work

This study was restricted to the available borecores provided from earlier exploration, and therefore the opportunity to drill boreholes to optimum depths in optimum locations was not available. Borehole D1 gave a good cross-section of lithologies, which captures much of the typical sequence.

Borehole D2, however, was terminated while still in the Main Zone, and so restricted opportunities to provide a more comprehensive assessment of the full Main Zone sequence, and the depth at which the Merensky Reef occurs. Extending this borehole to a similar depth to D1 may therefore capture that data. Further drill holes from this area should be analysed using the same techniques outlined in this study.

Geochemical and isotopic analyses, in particular, would offer a better understanding of how the units varied laterally, both along the strike to the dome and with distance away from the dome. Along the length of the borecore itself, the sampling density should be increased in order to constrain breaks and reversals, that may be present within sampling gaps.

APPENDIX 1: BOREHOLE LOG DESCRIPTIONS

BOREHOLE D1 LOG : Logged by Roger Scoon

Depth From	To	Depth* From	To	Width	Rock Type	Comments	Colour	Grain Size	Zone
0.00	8.00	240.00	232.00	8.00	OB	Quartzite Scree.			
8.00	66.30	232.00	173.70	58.30	MGT-G	Badly weathered with poor recovery and very broken. Typical magnetite gabbro with 10-20% magnetite and approximately equal abundance of pyroxene and plagioclase. Magnetite forms large anhedral grains that are probably partially cumulus.	D GR	C	UZ
66.30	66.70	173.70	173.30	0.40	F-PX	Well defined layer of pyroxenite (orthopyroxene dominant) with pegmatoidal texture in part. No evident magnetite but abundant disseminated base metal sulphides (pyrite, minor chalcopyrite).	D GR-GN	C	UZ
66.70	66.73	173.30	173.27	0.03	MGT	Well defined layer of Ti-magnetite with parallel contacts.	B	C	UZ
66.73	67.83	173.27	172.17	1.10	F-PX		D GR-GN	C	UZ
67.83	88.70	172.17	151.30	20.87	MGT-G	Includes poorly defined leucogabbronorite on the top contact. Abundant thin irregular magnetite stringers and local concentrations. Also abundant pyrite and chalcopyrite particularly on well developed joint planes.	D GR	C	UZ
88.70	90.50	151.30	149.50	1.80	F-PX	Well defined layer, although serpentinized. Sharp basal contact at 30°.	D GR-GN	C	UZ
90.50	93.60	149.50	146.40	3.10	SP-AN	Unusual texture and partially pegmatitic. Includes numerous cross cutting pegmatitic veins.	LT GR	C	UZ
93.60	95.00	146.40	145.00	1.40	MGT-G	Relatively low magnetite content (c. 10%) decreasing to less than 5% after 93m. Dark colour probably related to sausseritization of plagioclase.	D GR	C	UZ
95.00	111.72	145.00	128.28	16.72	L-G	Spotted anorthosite in places. Low magnetite content <5%. Graphic and pegmatoidal textures with a lot of recrystallization.	GR	C	UZ
117.72	125.20	128.28	114.80	13.48	MGT-G	Sharp upper contact of 50°. Magnetite content 5-10%. Foliation texture with elongated and orientated pyroxene grains. Trace amounts of sulphides at 123m.	D GR	MD	UZ
125.20	125.40	114.80	114.60	0.20	MGT	Well defined layer of Ti-magnetite with parallel contacts.	B	C	UZ
125.40	131.70	114.60	108.30	6.30	MGT-G	Altered and fractured in footwall to magnetite layer.	D GR	MD	UZ
131.70	136.21	108.30	103.79	4.51	G-N	Typical gabbronorite with 2 pyroxenes and approximately 5 % magnetite.	GR	MD	UZ
136.21	136.28	103.79	103.72	0.07	M-N	Well defined layer, but irregular contacts.	GR-GN	MD	UZ
136.28	137.43	103.72	102.57	1.15	G-N		GR	MD	UZ
137.43	138.64	102.57	101.36	1.21	M-N		GR-GN	MD	UZ
138.64	140.00	101.36	100.00	1.36	G	Mixed unit of gabbro and melanorite and intercalated pyroxenite.	D GR	C	UZ
140.00	142.00	100.00	98.00	2.00	F-PX		GR-GN	C	UZ
142.00	143.90	98.00	96.10	1.90	G		D GR	C	UZ
143.90	147.95	96.10	92.05	4.05	M-G	Complex zone of intercalated pyroxenite (unusually fine-grained) and gabbro, includes serpentinized zone at 147-148m.	GR-GN	MD-C	UZ
147.95	165.20	92.05	74.80	17.25	MGT-L-G	Plagioclase-rich which is unusual for magnetite gabbro. Magnetite approx 10%. Minor thin magnetite stringers and intercalated fine-grained pyroxenite layers. Recrystallized pegmatoidal texture associated with magnetite-rich layer. Impure magnetite layer at 155m.	GR	C	UZ
165.20	173.60	74.80	66.40	8.40	MT-AN	Trace amounts of disseminated magnetite. Two pyroxenes visible. Cumulus texture exhibited in "boulder" like forms of pyroxenite up to 10cm in diameter.	GR	MD	UZ
173.60	184.90	66.40	55.10	11.30	G-N	More typical gabbronorite with coarse blotchy texture which is characteristic of the Main Zone. No visible magnetite, two pyroxenes.	GR	C	UZ
184.90	185.00	55.10	55.00	0.10	F-PX		GR-GN	FN	UZ
185.00	203.00	55.00	37.00	18.00	M-N	Variable assemblage, in part pyroxenitic. Prominent cross-cutting plagioclase vein at 188-190.5m.	GR-GN	MD	UZ
203.00	232.07	37.00	7.93	29.07	G-N-PX	Mixed zone of gabbronorite, melanorite and pyroxenite. Intercalated and complex assemblage. Deformed with epidote-chlorite alteration.			UZ
232.07	240.50	7.93	-0.50	8.43	MGT-G	Melagabbro with abundant disseminated magnetite and thin magnetite stringers. Well defined impure magnetite layers at 233.78-233.85m and 234.14-234.16m. Magnetite layers and stringers oriented at 50°.		MD	UZ
240.50	248.80	-0.50	-8.80	8.30	L-G-N	No visible magnetite.	GR	MD	MZ
248.80	251.30	-8.80	-11.30	2.50	G-N	No visible magnetite.	GR	MD	MZ
251.30	252.00	-11.30	-12.00	0.70	MG-N		D GR	MD	MZ
252.00	261.60	-12.00	-21.60	9.60	L-G-N	Altered. Partially pegmatoidal texture and minor intercalated pyroxenite.	GR	MD	MZ
261.60	284.28	-21.60	-44.28	22.68	G-N	Typical Main Zone texture. Very altered.	GR	C	MZ
284.28	288.50	-44.28	-48.50	4.22	L-G-N	All orthopyroxene. Foliated texture defined at 50°. Very altered.	GR	MD	MZ
288.50	289.30	-48.50	-49.30	0.80	G-N	Very altered with chlorite and epidote.	GR	MD	MZ
289.30	294.50	-49.30	-54.50	5.20	SP-AN	Altered as above.	LT GR	C	MZ
294.50	302.80	-54.50	-62.80	8.30	L-G-N	Orthopyroxene grains 0.3-0.5cm. Grain size increases to large spots that resemble mottles, but cumulus and grading continues up into spotted anorthosite.	LT GR	C	MZ
302.80	312.23	-62.80	-72.23	9.43	MT-AN	Distinct layer of orthopyroxene with well defined mottles 1-1.5cm. Includes cumulus pyroxene from 308.10m and zone of deformation.	W	C	MZ
312.23	323.80	-72.23	-83.80	11.57	L-G-N	Foliated texture, predominantly orthopyroxene. Intercalated with impure anorthosite (partly mottled) layers. Weakly developed inch-scale layering at 30°.	LT GR	MD	MZ
323.80	324.40	-83.80	-84.40	0.60	G-N	In part feldspathic pyroxenite. Banding prominent due to deformation.	D GR	C	MZ
324.40	329.00	-84.40	-89.00	4.60	L-G-N	Deformation evident.	LT GR	MD	MZ
329.00	330.30	-89.00	-90.30	1.30	G-N		D GR	MD	MZ

Depth From	To	Depth* From	To	Width	Rock Type	Comments	Colour	Grain Size	Zone
330.30	334.55	-90.30	-94.55	4.25	G-N	Typical Main Zone blotchy texture. Intercalated anorthosite layers and melanorite "boulders".	GR	MD	MZ
334.55	336.00	-94.55	-96.00	1.45	G-N	Melanocratic.	D GR	C	MZ
336.00	348.25	-96.00	-108.25	12.25	G-N	As above. Partially leuconorite. Foliated texture.	GR	C	MZ
348.25	353.25	-108.25	-113.25	4.95	MT-AN	Irregular, medium sized (0.5-1cm) mottles which are probably orthopyroxene. Abr upper contact, although irregular.	W	MD	MZ
353.25	354.90	-113.25	-114.90	1.70	G-N	Gradational from above, very coarse grained with 0.5cm orthopyroxenes.	LT GR	C	MZ
354.90	363.50	-114.90	-123.50	8.60	MT-AN	As above, 0.5-1cm sized mottles. Towards the base, the mottles increase in size to over 1.5cm and in modal proportion to 25-30%	W	MD	MZ
363.50	398.20	-123.50	-158.20	34.70	G-N	Coarse grained, jointed and fractured with epidote, from 374-376m and 378-391m.	GR	C	MZ
398.20	429.35	-158.20	-189.35	31.15	MT-AN (GMA)	Distinct marker. Uppermost part comprises small (<0.5cm) rounded mottles, grading into zone of very coarse (>5cm), highly irregular mottles. Within deformation zone. From 420-425m layer of small mottles >425m coarse mottles.	W	V C	CUZ
429.35	429.65	-189.35	-189.65	0.30	L-N		LT GR	C	CUZ
429.65	430.50	-189.65	-190.50	0.85	MT-AN	Alteration with brittle deformation.	W	C	CUZ
430.50	432.18	-190.50	-192.18	1.68	N	Unusual texture with intercalated melanorite. Gradational into feldspathic pyroxenite at base. Altered.	LT GR	C	CUZ
432.18	435.20	-192.18	-195.20	3.02	L-N	Alteration in a shear zone.	LT GR	C	CUZ
435.20	436.10	-195.20	-196.10	0.90	N	Gradational upwards. Hanging wall to Bastard Reef.	LT GR	C	CUZ
436.10	436.59	-196.10	-196.59	0.49	F-PX (BR)	Includes well defined chromitite stringer (2mm thick) at base. Minor pegmatoid near base. Abundant (2%) base metal sulphides as composite grains (pyrrhotite, pyrite, chalcopyrite). Intersection angle at 60°.	GR-GN	C	CUZ
436.59	467.10	-196.59	-227.10	30.51	MT-AN	Sharp upper contact. Uppermost part comprises medium grained, irregular mottles (1-3cm). Below 468m, very felsic. Epidote-chlorite assemblage.	W	C	CUZ
467.10	468.37	-227.10	-228.37	1.27	L-N	Upper contact at 80° but irregular. Includes irregular layer of pegmatoidal norite from 467.8-467.85m.	LT GR	MD	CUZ
468.37	473.80	-228.37	-233.80	5.43	F-PX (MC)	Uppermost 1m is pegmatoidal and very feldspathic. Rest is partially pegmatoidal and all coarse grained. Thin (1mm) chromitite stringer at base. Evidence of a pot-hole.	GR-GN	C	CUZ
473.80	474.84	-233.80	-234.84	1.04	MT-AN	Includes irregular segregation of pyroxenite in uppermost 20cm.	W	C	CUZ
474.84	475.00	-234.84	-235.00	0.16	N	Minor base metal sulphides and micaceous.	LT GR	C	CUZ
475.00	476.80	-235.00	-236.80	1.80	MT-AN		W	C	CUZ
476.80	476.90	-236.80	-236.90	0.10	P-PX	Very thin, irregular chromitite stringer at base. Abundant base metal sulphides.	GR-GN	C	CUZ
476.90	480.67	-236.90	-240.67	3.77	MT-AN	Very felsic and coarse grained with 5-10cm mottles.	W	C	CUZ
480.67	485.05	-240.67	-245.05	4.38	F-PX (MP)	480.67 - 480.68m: Knife sharp upper contact with 2-3cm chromitite stringer at 60o. Matrix of chromitite essentially plagioclase. 480.68 - 481.60m: Typical coarse grained pyroxenite (non-pegmatoidal) with abundant base metal sulphides, which occur as classic composite grains, typically 0.2-0.5cm in diameter. 481.60 - 481.62m: Composite layer comprising two thin chromitite stringers at the top (1mm) and base (3mm) separated by a 1cm thick layer of anorthosite. 481.62 - 483.93m: Typical coarse grained pyroxenite (non-pegmatoidal) with abundant base metal sulphides (>2%) gradually decreasing to <1% towards base. 483.93 - 485.05m: Pegmatoidal pyroxenite with approximately 1% base metal sulphides. Upper and lower contacts gradational. No chromitite on base.	GR-GN	C	CUZ
485.05	488.28	-245.05	-248.28	3.23	N	Typically c.40% pyroxene. Minor fracturing. Sharp basal contact. Again no chromitite.	LT GR	MD	CUZ
488.28	492.11	-248.28	-252.11	3.83	P-PX	488.21 - 489.31m: Very coarse grained pegmatoidal pyroxenite with c.20% plagioclase. Distinctive texture with large (10cm) oikocrysts of clinopyroxene. Trace base metal sulphides. 489.31 - 489.48m: Norite with some recrystallisation. 489.48 - 490.36m: Pegmatoidal pyroxenite. Gradational contacts. 490.36 - 491.60m: Norite with irregular patches of pegmatoidal pyroxenite. 491.60 - 492.11m: Pegmatoidal pyroxenite.	GR-GN	C	CUZ
492.11	495.80	-252.11	-255.80	3.69	N	Typical but with irregular patches of pegmatoidal pyroxenite.	LT GR	MD	CUZ
495.80	497.50	-255.80	-257.50	1.70	L-N	Typical but with irregular patches of pegmatoidal pyroxenite.	LT GR	MD	CUZ
497.50	498.93	-257.50	-258.93	1.43	MT-AN		W	C	CUZ
498.93	506.30	-258.93	-266.30	7.37	N		LT GR	MD	CUZ
506.30	510.00	-266.30	-270.00	3.70	L-N		LT GR	MD	CUZ
510.00	515.00	-270.00	-275.00	5.00	N		LT GR	MD	CUZ
515.00	524.25	-275.00	-284.25	9.25	M-N P-PX	Mixed assemblage of intercalated norite and pyroxenite.	GR-GN	C	CUZ
524.25	529.00	-284.25	-289.00	4.75	N		LT GR	MD	CUZ
529.00	556.50	-289.00	-316.50	27.50	F-PX	Massive unit with only very minor jointing. Partially melanorite with up to 20% plagioclase.	GR-GN	C	CUZ
556.50	557.00	-316.50	-317.00	0.50	L-N		LT GR	MD	CUZ
557.00	557.50	-317.00	-317.50	0.50	M-N		GR	MD	CUZ

Depth From	To	Depth* From	To	Width	Rock Type	Comments	Colour	Grain Size	Zone
557.50	558.20	-317.50	-318.20	0.70	F-PX		GR-GN	C	CUZ
558.20	563.00	-318.20	-323.00	4.80	N	Unusual texture with coarse grains. Partially melanorite with thin pyroxenite layers.	LT GR	C	CUZ
563.00	565.00	-323.00	-325.00	2.00	M-N		GR	MD	CUZ
565.00	566.70	-325.00	-326.70	1.70	N		LT GR	C	CUZ
566.70	578.65	-326.70	-338.65	11.95	M-N	Very coarse grained from 571.45-578.65m.	GR	C	CUZ
578.65	580.20	-338.65	-340.20	1.55	N	Minor alteration and plagioclase veinlets.	LT GR	C	CUZ
580.20	582.40	-340.20	-342.40	2.20	M-N		GR	C	CUZ
582.40	584.44	-342.40	-344.44	2.04	N	Sharp basal contact with thin plagioclase layer.	LT GR	C	CUZ
584.44	584.77	-344.44	-344.77	0.33	F-PX		GR-GN	MD	CUZ
584.77	584.94	-344.77	-344.94	0.17	L-N		LT GR	MD	CUZ
584.94	585.10	-344.94	-345.10	0.16	F-PX		GR-GN	MD	CUZ
585.10	585.15	-345.10	-345.15	0.05	Q-F	Vein of quartz and feldspathic material.	W	MD	
585.15	586.85	-345.15	-346.85	1.70	N	Inch scale layering with melanorite bands. Intersection angle at 60°.	LT GR	C	CUZ
586.85	589.00	-346.85	-349.00	2.15	F-PX		GR-GN	MD	CLZ
589.00	589.56	-349.00	-349.56	0.56	CHR	Sharp upper contacts at 40°. Includes pyroxenite stringer from 589.26-589.33m. Lower contact irregular and pot-holed.	B	MD	MG
589.56	590.86	-349.56	-350.86	1.30	F-PX		GR-GN	MD	CLZ
590.86	591.88	-350.86	-351.88	1.02	CHR	Massive layer with sharp upper contact at 40°. Basal contact irregular.	B	MD	MG
591.88	592.05	-351.88	-352.05	0.17	CHR-PX	Abundant irregular chromitite stringers.	D GR	MD	CLZ
592.05	593.33	-352.05	-353.33	1.28	F-PX		GR-GN	MD	CLZ
593.33	593.41	-353.33	-353.41	0.08	CHR		B	MD	MG
593.41	593.57	-353.41	-353.57	0.16	F-PX		GR-GN	MD	CLZ
593.57	593.66	-353.57	-353.66	0.09	CHR		B	MD	MG
593.66	593.85	-353.66	-353.85	0.19	F-PX		GR-GN	MD	CLZ
593.85	593.87	-353.85	-353.87	0.02	CHR		B	MD	MG
593.87	594.13	-353.87	-354.13	0.26	F-PX		GR-GN	MD	CLZ
594.13	594.75	-354.13	-354.75	0.62	CHR	Massive layer with sharp upper contacts at 40°. Basal contact irregular.	B	MD	MG
594.75	594.98	-354.75	-354.98	0.23	F-PX		GR-GN	MD	CLZ
594.98	595.15	-354.98	-355.15	0.17	CHR		B	MD	MG
595.15	595.40	-355.15	-355.40	0.25	F-PX	Minor chromitite stringers. Intersection angles of layering are parallel in above sequence of chromitites.	GR-GN	MD	CLZ
595.40	635.80	-355.40	-395.80	40.40	F-PX	Massive except from 620.6-623m where broken and minor core loss. Prominent oikocrysts of clinopyroxene. A foliated texture is exhibited in parts.	GR-GN	MD	CLZ
635.80	637.43	-395.80	-397.43	1.63	CHR-PX	Minor chromitite stringers and with 0.5cm layer at 636.60m.	GR-GN	MD	CLZ
637.43	637.52	-397.43	-397.52	0.09	CHR	Intersection angles at 40°.	B	FN	LG
637.52	650.71	-397.52	-410.71	13.19	F-PX		GR-GN	MD	CLZ
650.71	650.79	-410.71	-410.79	0.08	CHR	Layered, parallel contacts at 40°. Massive chromitite.	B	FN	LG
650.79	654.54	-410.79	-414.54	3.75	F-PX		GR-GN	MD	CLZ
654.54	654.60	-414.54	-414.60	0.06	CHR	Minor pegmatoid in the hanging wall. Contacts rather irregular.	B	FN	LG
654.60	671.10	-414.60	-431.10	16.50	F-PX		GR-GN	MD	CLZ
671.10	671.18	-431.10	-431.18	0.08	CHR	Massive chromitite, parallel contacts at 45°.	B	FN	LG
671.18	744.95	-431.18	-504.95	73.77	F-PX	Minor shearing with sub-parallel fractures at 45°. Dolerite at 676.04-676.11m and 676.48-676.86m, sub-parallel to core. 682 - 687.5m: Fractured and broken, pyroxene serpentinized. 689.6 - 690m: Pegmatoidal pyroxenite, clearly recrystallized, rather altered. 695 - 698m: Serpentinized with abundant sub-parallel fractures at 30°. Also pegmatoidal pyroxenite in part. 733.19 - 733.22m: Irregular, pod like chromitite. 733.96 - 733.99m: Irregular chromitite layer. 739.1m: Irregular dissemination of chromitite in pyroxenite.	GR-GN	MD	CLZ
744.95	745.09	-504.95	-505.09	0.14	CHR	Well defined layer. Upper contact at 45° but lower contact irregular, with wedge of pyroxenite.	B	FN	LG
745.09	752.15	-505.09	-512.15	7.06	F-PX	Irregular and broken from 748.46-748.54m.	GR-GN	MD	CLZ
752.15	762.32	-512.15	-522.32	10.17	L-N	Sharp transition into spotted anorthosite / leuconorite. Initially includes minor bands of pyroxenite, but from 752.5m entirely noritic. Rather fractured and broken.	GR	MD	CLZ
762.32	772.04	-522.32	-532.04	9.72	F-PX		GR-GN	MD	CLZ
EOH	772.04m								

BOREHOLE D2 LOG : Logged by Tony Long

Depth From	To	Depth* From	To	Width	Rock Type	Comments	Colour	Grain Size	Zone
0.00	12.80	445.00	432.20	12.80	OB				
12.80	13.25	432.20	431.75	0.45	G		GR	MD	UZ
13.25	13.60	431.75	431.40	0.35	MGT	Euhedral cumulus feldspar laths and interstitial pyroxene.	BLK	MD	UZ
13.60	16.32	431.40	428.68	2.72	G		GR	MD	UZ
16.32	16.94	428.68	428.06	0.62	MGT	With included pegmatite veinlet at 70°.	BLK	MD	UZ
16.94	20.00	428.06	425.00	3.06	G		GR	MD	UZ
20.00	23.50	425.00	421.50	3.50	MGT-G	Euhedral feldspar laths present. Includes narrow magnetite layer.	D GR	MD	UZ
23.50	25.50	421.50	419.50	2.00	MGT-AN	Occasional interstitial chalcopyrite grains.	LT GR	MD	UZ
25.50	27.60	419.50	417.40	1.90	L-G		GR	MD	UZ
27.60	27.80	417.40	417.20	0.20	MT-AN	Sharp hanging wall contact at 75°.	W	MD	UZ
27.80	32.50	417.20	412.50	4.70	MGT	Sharp hanging wall contact. Some biotite.	D GR	MD	UZ
32.50	38.40	412.50	406.60	5.90	AN		GR	MD	UZ
38.40	39.70	406.60	405.30	1.30	PX		GR-GN	MD	UZ
39.70	43.10	405.30	401.90	3.40	F-PX		GR	MD	UZ
43.10	46.20	401.90	398.80	3.10	MGT-AN	Occasional interstitial sulphide grains.	LT GR	MD	UZ
46.20	48.50	398.80	396.50	2.30	MGT-AN		LT GR	MD	UZ
48.50	50.50	396.50	394.50	2.00	F-PX	Euhedral feldspar laths.	GR-GN	MD	UZ
50.50	52.40	394.50	392.60	1.90	MGT	Some biotite.	GR	MD	UZ
52.40	53.95	392.60	391.05	1.55	G		LT GR	MD	UZ
53.95	54.90	391.05	390.10	0.95	L-G		LT GR	MD	UZ
54.90	59.70	390.10	385.30	4.80	AN	Magnetite increases towards base.	LT GR	MD	UZ
59.70	59.90	385.30	385.10	0.20	MGT-AN	Grading downwards to impure magnetite.	D GR	MD	UZ
59.90	60.35	385.10	384.65	0.45	G		LT GR	MD	UZ
60.35	61.80	384.65	383.20	1.45	G-N	Feldspar laths display distinct fabric at 18-20°. Sharp hanging wall contact.	GR-GN	MD	UZ
61.80	66.40	383.20	378.60	4.60	G		GR	MD	UZ
66.40	69.20	378.60	375.80	2.80	MGT L-G		GR	MD	UZ
69.20	71.05	375.80	373.95	1.85	AN		LT GR	MD	UZ
71.05	73.00	373.95	372.00	1.95	MGT-AN		LT GR	MD	UZ
73.00	76.00	372.00	369.00	3.00	MGT-G		GR	MD	UZ
76.00	76.80	369.00	368.20	0.80	MGT-AN	Fairly sharp hanging wall contact.	D GR	MD	UZ
76.80	78.70	368.20	366.30	1.90	MGT-AN		LT GR	MD	UZ
78.70	79.20	366.30	365.80	0.50	MGT-AN		D GR	MD	UZ
79.20	79.81	365.80	365.19	0.61	MGT		BLK	MD	UZ
79.81	81.69	365.19	363.31	1.88	MT-AN	Coarse grained feldspar laths. Sharp hanging wall contact.	LT GR	MD	UZ
81.69	96.50	363.31	348.50	14.81	AN	Some magnetite and isolated sulphide grains. Sharp hanging wall contact.	D GR	MD	UZ
96.50	97.59	348.50	347.41	1.09	MGT	Some coarse feldspar laths in upper portion.	BLK	MD	UZ
97.59	103.80	347.41	341.20	6.21	AN	Rare disseminated sulphides. Sharp hanging wall contact at 60°	GR	MD	UZ
103.80	104.36	341.20	340.64	0.56	MGT-AN		GR	MD	UZ
104.36	108.70	340.64	336.30	4.34	AN	Magnetite content increases towards base. Rare disseminated sulphides.	D GR	MD	UZ
108.70	109.52	336.30	335.48	0.82	MGT	Feldspar laths in upper portion and narrow interlayered anorthosites.	BLK	MD-FN	UZ
109.52	114.26	335.48	330.74	4.74	MGT-AN	Rare interstitial sulphides. Sharp hanging wall contact at 15°.	LT GR	MD	UZ
114.26	119.20	330.74	325.80	4.94	G-N	Sharp hanging wall contact at 28°.	GR-BRN	MD	UZ
119.20	125.60	325.80	319.40	6.40	AN	Upper portion mottled. Pyroxene content increases towards base of unit.	D GR	FN-MD	UZ
125.60	134.00	319.40	311.00	8.40	L-G		D GR	MD	UZ
134.00	136.25	311.00	308.75	2.25	MT-AN		GR	MD	UZ
136.25	151.80	308.75	293.20	15.55	L-G-N	Rare coarse magnetite aggregates.	D GR	MD	UZ
151.80	153.50	293.20	291.50	2.50	MT-AN		D GR	MD	UZ
153.50	156.60	291.50	288.40	3.10	L-G		LT GR	MD	UZ
156.60	159.00	288.40	286.00	2.40	MT-AN		O W	MD	UZ
159.00	164.00	286.00	281.00	5.00	AN	Magnetite bearing with narrow intercalated pegmatite veins.	GR	MD	UZ
164.00	168.90	281.00	276.10	4.90	AN	Magnetite bearing.	GR	MD	UZ
168.90	169.18	276.10	275.82	0.28	P	Biotite on contacts at 30°.	W	V C	UZ
169.18	177.35	275.82	267.65	8.17	G	Occasional pegmatite veinlets.	GR	MD	UZ
177.35	177.95	267.65	267.05	0.60	P	Contact at 25°.	W	V C	UZ
177.95	182.79	267.05	262.21	4.84	G		GR	MD	UZ
182.79	183.05	262.21	261.95	0.26	P		W	V C	UZ
183.05	184.85	261.95	260.15	1.80	G		GR	MD	UZ
184.85	185.67	260.15	259.33	0.82	P	Contact at 30°.	W	V C	UZ
185.67	187.70	259.33	257.30	2.03	G		D GR	MD-FN	UZ
187.70	189.50	257.30	255.50	1.80	G		GR	MD	UZ
189.50	190.85	255.50	254.15	1.35	L-G		LT GR	MD	UZ
190.85	193.54	254.15	251.46	2.69	MT-AN		W	MD	UZ
193.54	198.10	251.46	246.90	4.56	G	Sharp hanging wall contact at 53°.	D GR	MD-FN	UZ
198.10	198.25	246.90	246.75	0.15	P	Biotite on contacts at 53°.	W	V C	UZ

Depth From	To	Depth* From	To	Width	Rock Type	Comments	Colour	Grain Size	Zone
198.25	212.08	246.75	232.92	13.83	G-N		D GR	MD-FN	UZ
212.08	212.40	232.92	232.60	0.32	G		GR	MD	UZ
212.40	214.19	232.60	230.81	1.79	SP-AN		O W	MD	UZ
214.19	214.26	230.81	230.74	0.07	MGT	Coarse chalcopyrite on hanging wall.	BLK	MD	UZ
214.26	236.48	230.74	208.52	22.22	G		D GR	MD-FN	UZ
236.48	237.80	208.52	207.20	1.32	P	Contact at 15°.	W	V C	UZ
237.80	256.00	207.20	189.00	18.20	G-N		D GR	MD-FN	UZ
256.00	256.95	189.00	188.05	0.95	MGT-G		BLK	MD-FN	UZ
256.95	257.12	188.05	187.88	0.17	MGT-G	Disseminated sulphide-pyrite?	BLK	MD-FN	UZ
257.12	266.25	187.88	178.75	9.13	G	Sharp hanging wall contact at 80°.	GR	MD-FN	UZ
266.25	268.00	178.75	177.00	1.75	MGT-P	Some disseminated sulphide.	D GR	V C	UZ
268.00	268.08	177.00	176.92	0.08	MGT-P	Abundant fine sulphide-chalcopyrite?	BLK	V C	UZ
268.08	268.63	176.92	176.37	0.55	MGT-P		BLK	V C	UZ
268.63	269.17	176.37	175.83	0.54	G		GR	C	UZ
269.17	269.30	175.83	175.70	0.13	MGT-P	Abundant fine intercumulus sulphide-chalcopyrite?	BLK	V C	UZ
269.30	278.73	175.70	166.27	9.43	MGT-AN	Narrow magnetite layers. Sharp hanging wall contact at 65°.	BLK	MD-FN	UZ
278.73	278.84	166.27	166.16	0.11	MGT	Irregular but sharp hanging wall contact at 85°.	BLK	MD	UZ
278.84	280.30	166.16	164.70	1.46	MGT-AN	Fine interstitial sulphide.	D GR	MD	UZ
280.30	292.40	164.70	152.60	12.10	MGT-G-N		LT GR	MD	UZ
292.40	292.60	152.60	152.40	0.20	MGT-G	Well developed fabric.	GR	MD	UZ
292.60	292.85	152.40	152.15	0.25	MGT	Coarse cumulus feldspar laths and some sulphides.	BLK	C	UZ
292.85	310.20	152.15	134.80	17.35	G		GR	C	UZ
310.20	311.40	134.80	133.60	1.20	G	Has numerous propylite filled fractures at 20°.	GR	C	UZ
311.40	333.50	133.60	111.50	22.10	G		GR	C	UZ
333.50	336.35	111.50	108.65	2.85	MGT-L-G-N	Strong fabric.		MD	UZ
336.35	337.90	108.65	107.10	1.55	G	No magnetite. Sharp hanging wall contact.	GR-GN	MD	UZ
337.90	339.19	107.10	105.81	1.29	MGT	Impure. Hanging wall contact.	D GR	MD	UZ
339.19	349.70	105.81	95.30	10.51	AN	No magnetite.	LT GR	C	UZ
349.70	352.50	95.30	92.50	2.80	AN	Vitreous, with euhedral, tabular feldspar laths.	D GR	C	UZ
352.50	360.40	92.50	84.60	7.90	G-N	Predominantly black orthopyroxene with rare green or honey clinopyroxene.	GR-GN	MD	UZ
360.40	364.70	84.60	80.30	4.30	AN	Vitreous, with euhedral, tabular feldspar laths.	D GR	C	UZ
364.70	368.80	80.30	76.20	4.10	AN		GR	C	UZ
368.80	373.50	76.20	71.50	4.70	AN	Vitreous.	D GR	C	UZ
373.50	378.15	71.50	66.85	4.65	MT-AN		LT GR	V C	UZ
378.15	385.70	66.85	59.30	7.55	L-G-N		LT GR	MD	UZ
385.70	392.00	59.30	53.00	6.30	AN	Euhedral, intercumulus feldspar, pyroxene and rare intercumulus magnetite.	LT GR	C	UZ
392.00	392.10	53.00	52.90	0.10	P	Contact at 25°.	W	V C	UZ
392.10	402.30	52.90	42.70	10.20	L-G-N	Tabular euhedral feldspar.	GR	MD	UZ
402.30	402.55	42.70	42.45	0.25	P	Biotite on contacts at 70°.	W	V C	UZ
402.55	413.34	42.45	31.66	10.79	L-G-N		GR	MD	UZ
413.34	414.90	31.66	30.10	1.56	AN	With euhedral feldspar.	GR	C	UZ
414.90	418.20	30.10	26.80	3.30	AN	With euhedral tabular feldspar and rare intercumulus magnetite.	LT GR	C	UZ
418.20	421.45	26.80	23.55	3.25	MT-AN	Mottles consist of magnetite oikocrysts.	LT GR	C	UZ
421.45	423.63	23.55	21.37	2.18	MGT-G	With narrow anorthositic layers.	D GR	MD	UZ
423.63	428.11	21.37	16.89	4.48	MT-AN	With pyroxene and magnetite oikocrysts. Sharp hanging wall contact.	LT GR	C	UZ
428.11	431.70	16.89	13.30	3.59	G-N	Single magnetite poik on hanging wall. Sharp hanging wall contact.	LT GR	MD	UZ
431.70	432.15	13.30	12.85	0.45	L-G	Sheared.	W	MD-FN	UZ
432.15	451.25	12.85	-6.25	19.10	G-N	Well developed fabric in places.	LT GR	MD	UZ/MZ
451.25	452.20	-6.25	-7.20	0.95	L-G		W	MD-FN	MZ
452.20	459.70	-7.20	-14.70	7.50	G	Fabric.	LT GR	MD	MZ
459.70	464.55	-14.70	-19.55	4.85	L-G		LT GR	MD	MZ
464.55	481.87	-19.55	-36.87	17.32	L-G-N	Strong fabric from mineral layering.	O W	MD	MZ
481.87	554.35	-36.87	-109.35	72.48	L-G-N		LT GR	MD	MZ
554.35	554.65	-109.35	-109.65	0.30	A	Carbonate alteration with sheared contacts.	GR-GN	FN	MZ
554.65	557.50	-109.65	-112.50	2.85	L-G	Altered.	O W	MD	MZ
557.50	560.55	-112.50	-115.55	3.05	G-N		GR	C	MZ
560.55	563.95	-115.55	-118.95	3.40	AN	Predominantly dark green clinopyroxene.	D GR	MD	MZ
563.95	565.90	-118.95	-120.90	1.95	AN	Predominantly black orthopyroxene.	D GR	MD	MZ
565.90	573.60	-120.90	-128.60	7.70	MT-AN	Dark green clinopyroxene mottles.	LT GR	MD	MZ
573.60	580.82	-128.60	-135.82	7.22	MT-AN	Black orthopyroxene mottles, rare clinopyroxene grains in groundmass.	D GR	MD	MZ
580.82	593.50	-135.82	-148.50	12.68	AN	Green clinopyroxene mottles.	GR	MD	MZ
593.50	595.75	-148.50	-150.75	2.25	MT-AN	Large mottles, with green clinopyroxene oikocrysts.	W	MD	MZ
595.75	597.47	-150.75	-152.47	1.72	SP-AN	Coarse discreet pyroxene grains, zoned from brown orthopyroxene core to green clinopyroxene rim.	W	MD	MZ
597.47	EOH								

KEY TO TABLE

A	Altered	B	Black	UZ	Upper Zone
AN	Anorthosite	BN	Brown	MZ	Main Zone
CHR	Chromitite	GN	Green	CUZ	Upper Critical Zone
F-	Feldspathic	GR	Grey	CLZ	Lower Critical Zone
G	Gabbro	W	White	MAR	Marginal Zone
L-	Leuco-				
M-	Mela-	LT	Light	LG	Lower Group (Chromitites)
MGT	Mangnetitite/Magnetite-rich	D	Dark	MG	Middle Group (Chromitites)
MT-	Mottled				
N	Norite	O	Off	GMA	Giant Mottled Anorthosite
OB	Over burden			BR	Bastard Reef
P-	Pegmatitic	C	Coarse	MC	Merensky Callboy
PX	Pyroxenite	FN	Fine	MP	Merensky Pyroxenite
Q	Quartz	MD	Medium		
SP-	Spotted	V	Very		

EOH	End of Hole
Depth*	Depth relative to the Upper Zone/Main Zone boundary

APPENDIX 2: PETROGRAPHIC DESCRIPTIONS

Borehole D1

121m (D1.119)
Plagioclase is the major cumulus phase with sub-euhedral shaped grains, ranging from 2mm to 9mm, aligned diagonally across the thin section. Small patches of alteration to sericite are found throughout the grains. Magnetite occurs as interstitial blebs that are continuous for up to 3mm as well as occurring as fine exsolution needles within pyroxenes, and as infill material along pyroxene grain fractures. Pyroxenes, both clinopyroxene and orthopyroxene, are intercumulus. The larger grains are mainly orthopyroxene, but grain sizes for both range from 1 - 4mm. An ophitic texture occurs where plagioclase grains are incorporated within pyroxenes. Minor alteration to chlorite is found at grain boundaries. A negligible amount of biotite is evident.

111m (D1.129)
Plagioclase is the major cumulus phase with grains between 1 - 3mm. It is present as an interstitial component, but the grains are smaller (< 0.5mm). Generally, grains are blocky, although a few elongate laths occur. Alteration to sericite is minor. Deformation of the plagioclase is slight. Magnetite is absent. Apart from one, relatively fresh, 0.5mm grain of clinopyroxene, almost all trace of pyroxene has been obliterated as a result of severe chloritisation.

102m (D1.138)
Plagioclase, in the form of euhedral laths ranging in length from 1 - 6mm, forms the major cumulus phase. Large patches of alteration to sericite are evident throughout the phase. Deformation is evident only in a small fraction of plagioclase grains as bent twinned lamellae. Magnetite occurs both as interstitial blebs up to 4mm in size, and as exsolution needles within the pyroxenes, which are < 0.1mm long. Clinopyroxene is the minor cumulus phase. The grains are sub-anhedral and range from 0.5 - 3mm. Alteration to chlorite affects all grains. At grain boundaries, biotite is found. Measuring < 1mm, it is associated with magnetite.

56m (D1.184)
Plagioclase, for the most part, forms the major cumulus phase with sub-euhedral grains, ranging in size from 1 - 4mm, which are clearly aligned. The remainder appears as a component of the interstitial groundmass, where grains are < 0.5mm. Myrmekitic texture is apparent in only one grain. Very small patches of sericitisation have attacked the majority of the grains. Evidence of minor deformation affecting occasional grains is exhibited in bent twins within the plagioclase. Magnetite occurs as interstitial blebs, ranging from 0.5 - 9mm, and as exsolution needles within pyroxene grains. Minor cumulus pyroxene is represented by very small amounts of clinopyroxene and inverted pigeonite. Both pyroxenes have sub-anhedral grains commonly < 2mm in size. Minor alteration to chlorite is noted throughout both minerals. Biotite is found in association with the chlorite and also magnetite.

45m (D1.195)
The major cumulus phase is plagioclase. Grains are sub-euhedral, measure from 1 - 5mm, and are aligned along the long axis of the thin section. Patches of alteration to sericite are seen throughout the sample. Minor deformation is observed in the slight bending of twins in plagioclase. Magnetite is present as interstitial blebs, commonly 2 - 3mm in length, and as exsolution needles within pyroxenes, < 0.1mm. The pyroxene component is dominated by clinopyroxene with only a few grains of inverted pigeonite occurring. Both minerals have sub-anhedral grains that fall between 1 - 3mm. Alteration to chlorite is

evident at grain boundaries. Biotite is mostly found associated with interstitial magnetite and is < 1mm in size.

16m (D1.224)
Plagioclase forms the major cumulus phase with sub-euhedral grains ranging from 1 - 5mm in size. Alteration is prevalent throughout the sample, often causing the grain boundaries to be indistinct. Deformation is absent. Magnetite is found as finely disseminated angular grains, no more than 2mm in size, in an interstitial role. Pyroxene is the minor cumulus phase. Only clinopyroxene is observed, and grains measure 1 - 2mm. As with the plagioclase, grain boundaries are unclear due to the alteration of the original mineral. Both epidote and chlorite alteration are evident throughout the grains. Small amounts of biotite, existing as needles < 0.5mm, are noted within the interstitial component as are minor quantities of quartz.

-9m (D1.249)
Plagioclase is the major cumulus phase, having randomly oriented grains that are predominantly blocky. Only a few elongate laths are noted. Grains measure 1 - 3mm. Alteration is absent. Minor deformation has caused plagioclase twinning to curve. Magnetite is absent. Pyroxene occurs as a minor cumulus phase with both clinopyroxene and orthopyroxene occurring as sub-anhedral grains of 1 - 2mm. Both minerals exhibit alteration to chlorite around grain boundaries, where associated biotite, appearing as laths measuring 0.5 - 2mm, is also recorded. A minor amount of quartz is found as an interstitial mineral.

-19m (D1.259)
Plagioclase constitutes not only the major cumulus phase, but also a large proportion of the interstitial fraction. Grains are generally sub-anhedral to anhedral and range in size from 0.5 - 2mm. Patches of sericite alteration are quite extensive. Deformation is absent. Magnetite is absent. Minor cumulus pyroxene grains of clinopyroxene and orthopyroxene are 1 - 3mm in size. Discernment of any original features, such as exsolution lamellae, is difficult due to the severe chloritisation in the centre of these grains. Original grain boundaries have undergone minor alteration to hornblende. Biotite is evident as an interstitial mineral, appearing as sub-euhedral grains ranging from 0.5 - 2mm in size.

-25m (D1.265)
The major cumulus fraction is made up of blocky plagioclase grains, ranging in size between 2 - 4mm. A large proportion of plagioclase measures < 0.5mm and forms the interstitial component. Alteration to sericite occurs within the randomly oriented grains. Deformation of plagioclase is noted. There is little evidence of zonation. Magnetite occurs only as a trace of finely disseminated needles. Pyroxene is present as an intercumulus phase with orthopyroxene and clinopyroxene forming sub-anhedral mottles of up to 4mm in diameter, and as minor cumulus phase, where a high proportion of grains measuring < 0.5mm are located. An ophitic texture is exhibited where mottles include grains of plagioclase. The majority of grains are altered to chlorite at their grain boundaries, but a few grains show more extensive alteration, so that only a small core of the original mineral remains. Biotite laths of < 1mm are also present in association with pyroxene and chlorite.

-31m (D1.271)
The major cumulus phase is formed by sub-euhedral plagioclase grains aligned across the thin section, that range from 0.5 - 3mm. Alteration to sericite is noted only in the larger grains, whereas deformation has resulted in bent twinning in the plagioclase throughout. Magnetite is absent. Pyroxene is present as an intercumulus phase. Clinopyroxene occurs more often than orthopyroxene, but both minerals have sub-anhedral grains which range from 0.5 - 4mm. An ophitic texture is exhibited frequently due to the

many plagioclase grains enclosed within the pyroxenes. Alteration to chlorite occurs around grain boundaries. Biotite grains of 0.5 - 3mm in size are associated with pyroxene and chlorite.

-36m (D1.276)
The majority of plagioclase is present as a major cumulus phase, but a minor proportion is a component of the interstitial groundmass. Grains are sub-euhedral, range in size from 0.5 - 4mm, and are randomly oriented throughout the thin section. Sericite alteration is found as small patches within grains and along fractures. Deformation is absent. Magnetite is absent. Pyroxene is represented by clinopyroxene as an intercumulus phase composing mottles of up to 4mm in diameter, enclosing plagioclase grains in an ophitic texture. Alteration to chlorite is extensive and secondary hornblende is observed. Small quantities of fine needles of biotite also occur.

-42m (D1.282)
Plagioclase is the major cumulus phase. The blocky grains are fragmented and range from 0.5 - 3mm. Alteration is evident as large patches of sericite throughout the grains. Deformation has caused plagioclase twins to bend. Magnetite is found as exsolution lamellae, < 0.1mm, within the pyroxenes. Pyroxene appears as the minor cumulus phase with clinopyroxene and orthopyroxene coexisting. Grains are 0.5 - 2mm and < 1mm respectively and have a sub-anhedral appearance. Extensive alteration to chlorite is evident along internal fractures and around boundaries. Biotite occurs widely and ranges from 0.5 - 2mm.

-48m (D1.288)
Interstitial plagioclase grains of < 0.5mm prevail. Larger major cumulus grains, between 1 - 2mm in size occur occasionally. Sericite alteration is prevalent. Deformation is absent. Magnetite is absent. Pyroxene is a minor cumulus phase, solely represented by orthopyroxene, which measure up to 2mm in diameter. The alteration process has obliterated most of the original internal structures of the grains and chloritisation is observed around their boundaries and along internal fractures. Minor amounts of biotite are present in an interstitial role with grains up to 2mm in size.

-51m (D1.291)
The thin section is highly altered and there is little evidence of original plagioclase grains. Magnetite is absent. Original pyroxene is apparent, with grains ranging in size from 1 - 5mm. Due to extensive sericitisation, chloritisation and epidotisation that has occurred throughout, the internal structures of the pyroxene are indeterminable. A minor amount of quartz is present. Biotite is absent.

-58m (D1.298)
Sub-euhedral shaped plagioclase grains are present only as the major cumulus phase and they range in grain size from 1 - 3mm. Evidence of deformation in plagioclase is in the form of bent lamellae. Alteration to sericite has occurred throughout the thin section, but is mainly confined to grain boundaries. Deformation is absent as is magnetite. Pyroxene appears as intercumulus, sub-anhedral mottles 1 - 4mm in size, with only orthopyroxene present. An ophititic texture is observed where grains include plagioclase. Minor chlorite alteration is noted at grain boundaries. A small quantity of euhedral biotite grains, measuring up to 0.5mm in size, are associated with both pyroxene and chlorite.

-64m (D1.304)
Plagioclase forms the major cumulus phase with sub-euhedral grains measuring up to 4mm. An interstitial component is also present, but the grains are finer, < 1mm. Partial alteration to sericite has occurred. Deformation is absent. Magnetite is absent. Pyroxene is represented solely by clinopyroxene as

sub-anhedral mottles ranging from 2 - 5mm in size. Ophitic textures are observed where pyroxene contains plagioclase grains. Minor alteration to chlorite is apparent around grain boundaries. Biotite is associated with pyroxene and chlorite. As needles of < 0.5mm in length, biotite also extends across the plagioclase grains.

-69m (D1.309)
Plagioclase is the major cumulus phase with sub-euhedral grains ranging up to 4mm. It is also a component of the interstitial groundmass, but grains are predominantly < 0.5mm. Patches of sericitisation are extensive throughout the sample. Deformation of albite twins has occurred within the cumulus plagioclase. Magnetite is absent. Clinopyroxene is the only pyroxene present and forms the intercumulus phase, which is optically continuous over large areas. One particular mottle is 10mm in diameter. Incorporated plagioclase grains result in an ophitic texture. Alteration to chlorite is prevalent within the cores and boundaries of clinopyroxene grains. Biotite, < 1mm in length, is also evident in minor proportions throughout the thin section.

-76m (D1.316)
Plagioclase is present both as a major cumulus phase, with sub-euhedral grains measuring 2mm, and as a considerable interstitial component, where the grains are < 0.5mm. Alteration to sericite and other clays is prevalent throughout all the grains, often obliterating any internal grain structures. Deformation, evident in only a few of the plagioclase grains. Magnetite is absent. Both clinopyroxene and orthopyroxene are present, forming the minor cumulus phase with grains ranging from 0.5 - 2mm. Internal structures are mostly destroyed by alteration to chlorite, making it impossible to identify sets of exsolution lamellae. Associated biotite occurs in moderate proportions.

-79m (D1.319)
Both major cumulus and a minor amount of interstitial plagioclase are present. Sub-euhedral grains ranging in size from < 0.5 - 3mm are randomly oriented. Small clusters of sericite alteration occur throughout the thin section. Deformation has been slight with only a few affected plagioclase grains. Magnetite is absent. Clinopyroxene is the only pyroxene present and sub-anhedral grains of < 1mm in size form a minor cumulus phase. The majority of grains exhibit moderate to severe alteration. Chlorite occurs within grains and at their grain boundaries. Associated biotite is present in negligible amounts as grains smaller than 0.5mm.

-81m (D1.321)
Sub-anhedral grains of plagioclase comprise the major cumulus phase and also a minor fraction of the interstitial material. Grain sizes are 1 - 3mm and < 1mm respectively. Small patches of sericite across the thin section provide evidence of minor alteration. Deformation has also occurred throughout the plagioclase. Magnetite is absent. Pyroxene is an interstitial phase, composed solely of sub-anhedral clinopyroxene grains, which measure 1 - 2mm. A sub-ophitic texture is observed where plagioclase grains are incorporated. Minor alteration to chlorite occurs at the boundaries and is associated with small amounts of biotite grains, which are 0.5 - 1mm in size.

-82m (D1.322)
Major cumulus and interstitial plagioclase occurs with sub-euhedral to sub-anhedral grains measuring 1 - 2mm and < 1mm respectively. Alteration to sericite is minimal and deformation is confined to only a few grains. Magnetite is absent. Pyroxene is intercumulus only, composed of clinopyroxene and orthopyroxene. The majority of grains are between 1 - 2mm, though mottles are optically continuous up to 5mm. A sub-ophitic texture between incorporated plagioclase grains and the pyroxenes is noted.

Alteration to chlorite is found at grain boundaries only. Fine needles of biotite are found throughout the section.

-85m (D1.325)
A major cumulus is present, but the greater proportion of plagioclase grains, which are sub-euhedral and < 1mm in size, are interstitial. Minor alteration to sericite is noted in only a few grains. Deformation is absent, as is magnetite. Pyroxene occurs as clinopyroxene and orthopyroxene in an intercumulus role. Orthopyroxene occurs as mottles, optically continuous up to 6mm, whereas the clinopyroxene occurs as grains of < 1mm. A sub-ophitic texture exists between the orthopyroxene and the plagioclase grains held within the mottles. Minor alteration to chlorite is noted at grain boundaries. Biotite is evident throughout as fine grains in association with the chlorite.

-87m (D1.327)
Both major cumulus and interstitial plagioclase are present with grains varying from 0.5 - 2mm in size. The major cumulus grains are blocky in shape. Sericite alteration is confined to the interstitial component. Deformation is evident within the grains where albite twins in the plagioclase appear slightly bent. Clinopyroxene and orthopyroxene appear as the interstitial component, enclosing plagioclase grains in mottles < 2mm, creating an ophitic texture. Minor alteration to chlorite is found around the majority of the pyroxene grains. The larger grains are highly fractured with alteration also occurring along these breaks. Biotite is evident throughout, with grain size commonly in excess of 1mm.

-92m (D1.332)
Plagioclase is the major cumulus phase, with sub-euhedral to sub-anhedral grains that range in size from 1 - 5mm. A moderate amount of alteration to sericite occurs throughout the thin section. Minor evidence for deformation exists in the plagioclase. Minor cumulus clinopyroxene and orthopyroxene are present as 1 - 4mm sub-anhedral grains. Chlorite alteration is located at the edges of the pyroxene grains. Biotite, is found associated with the chlorite, and is present as euhedral grains 0.5 - 2mm in length.

-98m (D1.338)
Major cumulus plagioclase grains vary in size between 1 - 3mm. Only a minor interstitial plagioclase component is present at this depth. Alteration is minor, with the majority of the grains appearing fresh. Deformation is rife, with many of the grains exhibiting bent albite twins. Pyroxenes occur as the minor cumulus phase with grains ranging in size from 0.5 - 3mm. Clinopyroxene is commonly larger than the orthopyroxene. Minor chlorite alteration is found at pyroxene rims. Deformation is evident in the pyroxenes, where the exsolution lamellae are curved in appearance. Biotite up to 2mm in length is evident throughout.

-108m (D1.348)
Only major cumulus plagioclase is found at this depth. The plagioclase grains in this sample vary in size from 1 - 3mm. The smaller grains appear to be more susceptible to alteration to sericite. Minor deformation of plagioclase exsolution lamellae is noted to occur. Intercumulus pyroxenes, in the form of both clinopyroxene and orthopyroxene, exhibit a sub-ophitic texture with the plagioclase. Pyroxene grain size is commonly between 2 - 4mm. Chlorite alteration is evident within the grain and at grain boundaries. Biotite also occurs throughout the sample, up to 2mm long.

-115m (D1.355)
Both interstitial and major cumulus plagioclase grains are found at this depth. The majority of the grains appear sub-anhedral and range up to 4mm in length. Patchy alteration to sericite is evident across the thin section. Slight deformation is observed to occur in the plagioclase. Magnetite is found as exsolution

needles incorporated within the pyroxene grains. The majority of the intercumulus pyroxene is represented by clinopyroxene, with grain size ranging from 1 - 5mm. An ophitic texture exists between the pyroxenes and the plagioclase. Alteration rims of chlorite occur around the pyroxenes. Chlorite is also present in fractures and cracks within the center of the pyroxene grains. Deformation in the form of bent exsolution lamellae is seen in a small portion of the pyroxenes. Biotite grains, less than 2mm long are also present, and are found associated with the chlorite.

-121m (D1.361)
Plagioclase is represented by both the major cumulus phase and as interstitial material. Grains range in size between 0.5 - 3mm. Sericite alteration is found across the minor interstitial component and at the grain boundaries of the larger, cumulus plagioclase grains. Minor deformation is evident in only a minor proportion of the larger grains. Clinopyroxene and orthopyroxene grains, representing the intercumulus portion, are similar in their size, ranging between 0.5 - 2mm. A sub-ophitic texture is evident between the pyroxenes and the plagioclase. Alteration to chlorite is found in moderate amounts, with few of the grains more extensively affected than others. Biotite is present in small amounts, and commonly 1 - 2mm in length.

-128m (D1.368)
Major cumulus plagioclase grains are between 1 - 3mm in length. A minor portion of interstitial plagioclase is generally < 0.5mm long. Alteration and deformation are absent. Both clinopyroxene and orthopyroxene occur as the intercumulus phase. Grains are commonly between 2 - 4mm in length with a small percentage found between 0.5-1mm. An ophitic texture between the pyroxenes and plagioclase is present. Fracturing is common throughout the pyroxenes and alteration is present along these breaks as chlorite. Biotite, associated with the chlorite, occurs as small needles in minor amounts at the pyroxene grain boundaries.

-133m (D1.373)
Original grains at this depth have been altered to both clays and chlorite. Little remains of original grain structures and inter-grain relationships. Quartz veins cut through the thin section.

-134m (D1.374)
The larger, major cumulus grains are commonly 2mm in length and sub-euhedral in shape. These grains have been highly altered to sericite so that internal structures are difficult to distinguish. The minor portion of interstitial plagioclase is less affected by this alteration. Deformation is absent. Both pyroxenes, clinopyroxene and orthopyroxene, range in size between 0.5 - 3mm. An ophitic relationship between the pyroxenes and plagioclase is observed. Alteration at the pyroxene rims to chlorite is rife, with more pervasive alteration along fractures within the pyroxene grains. Alteration to hornblende at pyroxene grain boundaries is also extensive. Primary hornblende is also found to occur alongside the secondary hornblende, both approximately measuring 2mm in diameter. Biotite needles occur, associated with the pyroxenes in negligible amounts. Quartz occurs alongside the plagioclase in the interstitial portion.

-140m (D1.380)
Major cumulus plagioclase grains are sub-euhedral and 1 - 3mm long. Alteration to sericite is minor. Deformation is present in the plagioclase and occurs in many of the cumulus grains. Intercumulus clinopyroxene and orthopyroxene occur as large mottles < 4mm, presenting an ophitic texture. Orthopyroxene is the most abundant pyroxene. Minor alteration to chlorite is present at grain boundaries. Bent exsolution lamellae is evidence for deformation. Biotite needles which are 0.5 - 2mm in length are associated with chlorite alteration.

-144m (D1.384)
Both major cumulus and interstitial plagioclase are apparent at this depth. Grains range from < 0.5 - 3mm in length. Minor sericite alteration is apparent. Deformation of cumulus plagioclase grains is minor. Zonation is only present several of the grains. Magnetite exsolution, < 0.5mm in diameter, is seen within the pyroxene grains. Both orthopyroxene and clinopyroxene are present in the minor cumulus role. The grains, which are up to 2mm in diameter, are highly fractured and altered, with no remaining internal structures. Biotite, up to 2mm long, is found in minor amounts throughout the thin section.

-156m (D1.396)
Both plagioclase and pyroxene are evident but no cumulus/intercumulus phases can be discerned. Grain sizes for the plagioclase are in the region of 0.5 - 3mm. Alteration to sericite and clays of the plagioclase is prevalent. Deformation is absent. Pyroxenes reach 5mm in diameter. Internal structures are highly altered to chlorite, with no evidence available to indicate whether both clinopyroxene and orthopyroxene are in fact present. Biotite is absent. Quartz is evident throughout the sample.

-159m (D1.399)
Major cumulus plagioclase grains are 1 - 4mmin length. Only minor alteration to sericite occurs within the plagioclase grains. Deformation occurs within the plagioclase, which exhibit bent twinning. Clinopyroxene appears with inverted pigeonite, both of which are present in an intercumulus role. Single grains of clinopyroxene reach up to 10mm in diameter and form mottles enclosing plagioclase in a sub-ophitic texture. Inverted pigeonite grains average between 1 - 3mm. Negligible alteration of the pyroxenes to chlorite is present at grain boundaries. No biotite is observed in this thin section.

-176m (D1.416)
Plagioclase is present as a major cumulus mineral with grains varying in size up to 3mm. Alteration and deformation are both absent. Clinopyroxene exists alongside inverted pigeonite, both in an intercumulus role, with grain sizes < 1mm. Chlorite alteration is negligible. Minor amounts of biotite are present, typically as fine grained blebs throughout the thin section and with a single large grain, 2mm long.

-179m (D1.419)
Major cumulus plagioclase grains occurs with a minor proportion of intercumulus plagioclase, with the total variation in grain size 0.5 - 3mm. Alteration to sericite and other clays only exists in a small portion of the sample. Minor deformation of the twinning in the plagioclase is evident. The pyroxenes, both clinopyroxene and orthopyroxene, are intercumulus. They are generally found to occur as optically continuous mottles, < 5mm. These mottles are extensively fractured and altered around the margins to chlorite. Chlorite alteration is minor occurring across the pyroxenes. Biotite, associated with the chlorite, occurs as needles less than 0.5mm in length.

-182m (D1.422)
Major cumulus plagioclase grains are < 2mm in length, with interstitial grains generally < 0.5mm in size. There is little evidence of alteration to sericite. Deformation is found in the form of curved twinning in the plagioclase. Both clinopyroxene and orthopyroxene occur as intercumulus minerals, enclosing plagioclase within mottles, that reach 3mm in diameter. Alteration to chlorite is minor and only found at the grain boundaries of the pyroxenes. Minor biotite is also found as tiny needles throughout the thin section.

-184m (D1.424)
Plagioclase is the major cumulus phase, with grains 2 - 5mm in size. Alteration is absent. Deformation of twinning is apparent in the plagioclase, but is confined to only a few grains. Both clinopyroxene and orthopyroxene are present as the intercumulus phase. Both pyroxenes form large mottles, up to 17mm in diameter. These mottles exhibit an ophitic texture with the plagioclase. The rims of the pyroxene grains are commonly altered to chlorite. Negligible biotite is found.

-186m (D1.426)
A small proportion of all plagioclase is the major cumulus phase where grains reach 2mm. The majority of plagioclase grains are interstitial and < 0.5mm in size. Alteration to sericite is observed only within the interstitial component. Deformation, exhibited by bent twins within the plagioclase, is minor at this depth. Clinopyroxene and orthopyroxene are intercumulus, with a grain size < 0.5mm. The pyroxenes are mostly altered and fractured with chlorite present throughout the grains. Negligible biotite is observed in association with the chlorite.

-189m (D1.429)
Large cumulus grains of plagioclase, 2mm in length, appear as blocky remnants of larger grains. Large areas of alteration to clays are present throughout. Very few grain boundaries are clearly recognized due to alteration and fracturing. Deformation is absent. Clinopyroxene is the sole pyroxene, representing the intercumulus phase. Grains are less fragmented than the plagioclase and mottles enclosing plagioclase attain a maximum diameter of 5mm. Alteration to chlorite is prominent. No orthopyroxene is observed to exist at this depth. Biotite is found in negligible quantities. Quartz is present in small proportions.

-190m (D1.430)
Major cumulus plagioclase represents a small proportion of the entire thin section, with the majority of plagioclase represented by the interstitial component. Grain sizes are in the order of 0.5 - 2mm. Alteration to sericite is prevalent affecting the whole thin section. Deformation is absent. The only pyroxene present is clinopyroxene, which is found in a minor cumulus role. Grains vary in size between 0.5 - 3mm in diameter. Chlorite alteration is absent, as is biotite. Minor quartz is observed in this depth.

-193m (D1.433)
Major cumulus plagioclase grains are approximately 2mm in length. The interstitial portion, which represents the majority of the plagioclase, has a grain size of < 0.5mm. This fine grained fraction is more susceptible to alteration to sericite, which is consequently rife throughout the sample. Deformation is absent. Orthopyroxene is present as the minor cumulus phase, along with a minor amount of clinopyroxene. Grain sizes for both pyroxenes are < 4mm. Alteration to chlorite is also prevalent and obscures internal grain structures. No biotite is present.

-194m (D1.434)
Plagioclase is the major cumulus phase with grains up to 2mm in length. There is a minor proportion of plagioclase within the interstitial fraction. Alteration and deformation are both absent. Orthopyroxene and clinopyroxene are both observed in an intercumulus role. Mottles are seen containing fine grained plagioclase in an ophitic texture. Grain sizes vary between 1 - 3mm. Alteration to chlorite within pyroxenes and along fractures in the grains is extensive. Minor biotite appears as fine grained laths < 0.5mm long.

-195m (D1.435)
Plagioclase is the major cumulus phase, with blocky grains < 3mm in length. A moderate proportion of interstitial plagioclase is also present. Small patches of sericite alteration occur across the thin section. Deformation is absent. Both clinopyroxene and orthopyroxene are observed in minor cumulus roles, with grains < 3mm in size. Minor alteration to chlorite exists around the grain margins of the pyroxenes. A single grain of the orthopyroxene exhibits deformed exsolution lamellae. Biotite appears as 0.5 - 2mm long grains throughout the section.

-196m (D1.436)
Plagioclase grains are the major cumulus phase in this sample, with grains varying between 0.5-3mm in size. Minor alteration to sericite is observed in small patches. Deformation occurs as curved twinning in several of the larger grains of plagioclase. No clear evidence for original pyroxenes is evident in this sample, but chlorite alteration is apparent in minor amounts within the interstitial portion. Biotite is also present in small amounts, as grains < 1mm long, within the interstitial fraction. Chromite appears as very fine grained cubes, disseminated throughout the entire thin section and enclosed within plagioclase. This represents a cumulus phase.

-197m (D1.437)
Plagioclase is a major cumulus phase with many of the grains stubby in appearance, measuring < 2mm. Interstitial plagioclase grains are also evident. Alteration is extensive throughout the sample. Both grain boundaries and the internal grain structures have been obliterated. Minor deformation of the plagioclase lamellae is observed within the less altered portions of individual grains. Only clinopyroxene is seen in an intercumulus mineral, which is commonly < 0.5mm in size and altered to chlorite. Biotite and quartz occur in the interstitial groundmass. Tiny chromite cubes are present as a cumulus mineral. It is finely disseminated throughout the section, incorporated within both plagioclase and pyroxene grains.

-201m (D1.441)
The plagioclase component is a major cumulus phase. Grains are < 2mm in size. Alteration of the plagioclase to sericite and deformation is minor. The sole pyroxene is orthopyroxene, which is found to in an intercumulus role, < 1mm in diameter. Chlorite rims occur around the orthopyroxene margins. Tiny chromite cubes represent a cumulus phase and are evident throughout the thin section. A vein of alteration cuts across the thin section and is infilled with a fibrous form of chlorite and a minor amount of biotite.

-202m (D1.442)
Plagioclase is the major cumulus phase at this depth, with a large proportion of interstitial plagioclase also present. Grain sizes vary up to 3mm. Minor alteration to sericite is noted throughout the thin section. Deformation is absent. Only remnants of a few grains of clinopyroxene and orthopyroxene, in an intercumulus role, are identified. Alteration to chlorite is so extensive that no original internal structures remain. A minor amount of quartz coexists with the interstitial plagioclase. Both biotite and chromite are absent.

-214m (D1.454)
Major cumulus plagioclase grains are 0.5 - 2mm in length. Alteration is absent. Deformation of the plagioclase is evident in a few of the grains, where the twinning is bent. Fine fractures are found throughout the plagioclase. Both clinopyroxene and orthopyroxene occur within the intercumulus portion of the thin section, as < 0.5mm grains. Alteration to chlorite at grain boundaries is moderate. Cubes of cumulus chromitite, 0.5mm across, occur throughout the sample. Biotite is absent.

-215m (D1.455)
Major cumulus plagioclase grains are < 3mm in size. Interstitial plagioclase also occurs. Alteration to sericite occurs in patches. Deformation is distinguished in only a few grains, where twinning within the plagioclase are curved. Both clinopyroxene and orthopyroxene occur in an intercumulus role, with orthopyroxene proportionately greater in amount compared to clinopyroxene. Both types range in size from 0.5 - 2mm. The pyroxenes are mostly altered to chlorite, which has destroyed the grain boundaries and overprinted the majority of the original internal structures. Disseminated chromite cubes are seen throughout as a cumulus mineral. Negligible biotite is observed.

-218m (D1.458)
Major cumulus plagioclase is present, with grains ranging in size from very fine grained to 3mm. Alteration to sericite is prevalent. Deformation is of the plagioclase grains is extreme. Clinopyroxene is present as the sole pyroxene, in an intercumulus role. Grains are in the order of 1-3mm. Alteration to chlorite is extensive and minor biotite is found associated with this mineral. Disseminated chromite cubes are present throughout, as a cumulus phase, and are less than 0.1mm in diameter.

-220m (D1.460)
Plagioclase is the major cumulus mineral. The grains, commonly < 2mm long, are highly altered to sericite, and also highly fractured. Minor interstitial pyroxene occurs, where grains are < 0.5mm in diameter. Alteration to chlorite has destroyed the internal structures of the pyroxenes making the process of distinguishing between clinopyroxene and orthopyroxene impossible. Both biotite and chromite are absent.

-224 (D1.464)
Major cumulus plagioclase occurs as laths up to 4mm long. Interstitial plagioclase is generally < 0.5mm. Alteration and deformation are absent. The orthopyroxenes, 1 - 4mm in diameter, are generally larger than the clinopyroxenes which are only 1 - 2mm in diameter. Both pyroxenes are intercumulus, and enclose plagioclase grains within mottles, presenting a sub-ophitic texture. Both pyroxenes exhibit alteration around the grain margins to chlorite. Minor biotite is observed to exist in an interstitial manner. Needles of chromite are evident throughout the thin section and is a cumulus phase.

-227m (D1.467)
Major cumulus plagioclase grains are < 1mm. Alteration and deformation are absent. Both pyroxenes are present in an intercumulus role. Clinopyroxene and orthopyroxene grains are large, < 5mm in diameter. Both display an ophitic texture with the plagioclase. Negligible chlorite alteration is found, and only minor amounts of fine grained biotite occur. Chromite is a cumulus phase at this depth, which is disseminated throughout the section. Quartz is also apparent within the groundmass.

-228m (D1.468)
Plagioclase is present in a major cumulus role, where grains are < 3mm in length. A minor interstitial component coexists. Alteration to sericite is negligible. Deformation is seen to exist in some of the grains, where the twinning is bent. Both clinopyroxene and orthopyroxene exist at this level as the intercumulus phase and are approximately 2mm in diameter. A minor amount of fine grained plagioclase are found partly enclosed within the pyroxenes, exhibiting a sub-ophitic texture. Little alteration to chlorite around the grain boundaries occurs. Negligible amounts of fine grained biotite exist. Chromite is absent.

-236m (D1.476)
Major cumulus plagioclase occurs as grains < 2mm long. Alteration and deformation are absent. A relatively high proportion of all plagioclase is interstitial. Clinopyroxene occurs as the sole pyroxene in an intercumulus role, exhibiting a sub-ophitic texture with the plagioclase. Grain sizes vary between 1 - 2mm. Alteration around grain margins to chlorite is common. Biotite is closely associated with the chlorite and clinopyroxene. Disseminated chromite is observed and is a cumulus phase.

-257m (D1.497)
Plagioclase is the major cumulus phase, with grain sizes varying from 0.5 - 3mm. Alteration and deformation are absent. Orthopyroxene is the only pyroxene present, and is intercumulus. A sub-ophitic texture with the plagioclase occurs, with pyroxene mottles < 3mm. Portions of the mottles show alteration to chlorite around the rims of the individual fragments. Biotite is present within the interstitial portion in minor amounts. Chromite is absent.

-274m (D1.514)
Major cumulus plagioclase occurs alongside a small proportion of intercumulus plagioclase. Grains sizes are small, commonly < 1mm long. Alteration is absent, but deformation of plagioclase twinning is observed in a few of the larger grains. Ophitic textures are observed between the plagioclase and the pyroxenes. Both clinopyroxene and orthopyroxene are found in an intercumulus role, and vary between 0.5 - 3mm in diameter. Alteration of the rims of the pyroxenes to chlorites is evident with some grains more extensively altered than others. Biotite and chromite are both absent.

-298m (D1.538)
Small laths, < 1mm long, of major cumulus plagioclase constitute the majority of this section. Alteration and deformation are absent. Both clinopyroxene and orthopyroxene occur as 1 - 3mm intercumulus grains. Alteration to chlorite at grain boundaries and within fractures through the grains is minor. A few grains of plagioclase are incorporated within the pyroxenes producing a sub-ophitic texture. Biotite is absent. Finely disseminated chromite is apparent throughout the sample and is a cumulus phase.

-316m (D1.556)
Major cumulus plagioclase, 2mm in length, is present alongside a fine grained, interstitial fraction. Alteration and deformation are absent. Only orthopyroxene is present within this thin section, as an intercumulus phase, with grains attaining 3mm in diameter. A sub-ophitic texture is observed between the plagioclase and the pyroxene grains. Alteration to chlorite is negligible. Deformation of the pyroxene grains is evident in the exsolution lamellae, which is wavy in appearance. A negligible amount of fine grained biotite is observed. Chromite is absent.

-338m (D1.578)
Plagioclase represents the major cumulus phase, but grains are generally small, < 1mm. Minor alteration patches of sericite occur throughout the sample. Deformation is absent. Both pyroxenes are present as the intercumulus phase, the majority are represented by orthopyroxene, with minor amounts of clinopyroxene evident. The larger grains are 3mm in size. Both clinopyroxene and orthopyroxene exhibit an ophitic texture with plagioclase. Alteration to chlorite occurs along the fractures within the grains and in minor amounts around the pyroxene grain boundaries. Minor biotite also occurs, with grains averaging between 1-2mm in size. Chromite is absent.

-357m (D1.597).
Plagioclase is the major cumulus phase, with grains < 2mm long. Alteration is absent, but the deformation of twinning within the plagioclase grains is clear. Clinopyroxene and orthopyroxene are

intercumulus, with orthopyroxene occurring in greater amounts, with grains up to 10mm in diameter. An ophitic texture is observed. Minor chlorite alteration is present at grain boundaries. Deformation is evident where the exsolution lamellae appear wavy. Negligible biotite is present. Fine grained cubes of chromite are disseminated across the thin section and as a cumulus mineral.

Borehole D2

418m (D2.27)
Plagioclase is present both as a major cumulus phase and as an interstitial component of the matrix. Grain size ranges from 1 - 6mm and grain shape is sub-euhedral to sub-anhedral. Patches of sericite, observed within grains, indicate alteration has occurred. Deformation has caused the albite twins in the plagioclase to bend. Myrmekitic textures occur in a few of the smaller interstitial plagioclase crystals. Magnetite is a minor cumulus mineral and appears as either angular grains up to 5mm in diameter or as exsolution needles < 0.1mm. Pyroxene is represented solely by clinopyroxene, which forms a minor cumulus phase. Grains are sub-anhedral in appearance and measure 0.5 - 4mm. Minor alteration to chlorite occurs along internal grain fractures and at grain boundaries. Biotite is present as very small grains < 0.2mm in length.

405m (D2.40)
Plagioclase exists solely as a major cumulus phase, consisting mainly of fractured sub-euhedral to sub-anhedral remnants. These measure 2 - 7mm and include elongate laths. Minor alteration to sericite is found at the edges of some grains. Deformation is also evident as bent albite twins. Magnetite is a minor cumulus phase and appears in two forms: as 1mm diameter rounded blebs in association with biotite, and as exsolution needles within pyroxene grains. Pyroxene forms the minor cumulus fraction with clinopyroxene occurring more frequently than inverted pigeonite. Grains are < 2mm and 1 - 3mm respectively. Alteration of the clinopyroxene to chlorite is evident. Biotite occurs as an interstitial component with grains measuring < 1mm. It is often found associated with magnetite.

384m (D2.61)
Plagioclase forms both a major cumulus phase and a very small fraction of the interstitial component. The majority of the grains are large, measuring up to 5mm, and are sub-euhedral to sub-anhedral in shape. Alteration is absent. Albite twins are bent, indicating deformation of the plagioclase has occurred. Magnetite appears only as euhedral exsolution needles of < 0.1mm, which show sub-parallel alignment within the exsolution lamellae of pyroxene. Three pyroxenes are noted to form the minor cumulus fraction: primary clinopyroxene, orthopyroxene and inverted pigeonite. The latter is weakly pleochroic and has three obvious sets of exsolution lamellae when compared with the primary orthopyroxene. Grain sizes range from 1 - 3mm, 0.5 - 2mm and 2 - 4mm respectively and all have a sub-anhedral appearance. Minor chlorite alteration occurs as small exsolution needles throughout the pyroxenes. Biotite occurs as small grains that are < 0.1mm and found associated with magnetite.

329m (D2.116)
Plagioclase occurs as a major cumulus phase only. Grains are sub-euhedral to sub-anhedral and range in size from 1 - 6mm. Alteration has resulted in small patches of sericite within grains. Only minor deformation is noted in the plagioclase with slight zonation at grain margins. Magnetite is present mainly as euhedral needles of < 0.1 - 4mm within the exsolution lamellae of the pyroxenes. A single bleb of magnetite measuring 4mm in diameter also occurs. Both clinopyroxene and inverted pigeonite are present as a minor cumulus phase with sub-anhedral shaped grains of < 2mm and 1 - 4mm respectively. Minor alteration to chlorite occurs along internal grain fractures. Biotite is found associated with magnetite and is present as small grains less than 0.1mm in length.

298m (D2.147)
Plagioclase exists solely as a major cumulus phase and is composed of a predominantly blocky section of coarse grains, which measure 3 - 7mm including elongate laths. Small patches of alteration to sericite are found throughout the mineral. Deformation of the albite twins in the plagioclase is mild and only affects 10% of the grains. Magnetite occurs as exsolution within the pyroxene, and is frequently associated with

small amounts of biotite. It is present as euhedral needles which are < 2mm in size. Pyroxene appears as an intercumulus phase and has an ophitic texture, due to the inclusion of small grains of plagioclase. Large mottles of primary orthopyroxene, optically continuous up to 11mm, coexist with clinopyroxene and inverted pigeonite grains measuring 1 - 5mm and 1 - 2mm respectively. Chloritisation is minor and mostly confined to grain boundaries. Alteration is moderate along internal fractures, but more severe in the centre of one particular pyroxene grain, which is surrounded by secondary hornblende. Grains of inverted pigeonite exhibit large bleb-like lamellae of augite. Biotite, in the form of acicular grains of < 0.1mm, is found in minor amounts at pyroxene grain boundaries.

241m (D2.204)
Plagioclase appears both as large, though mainly indistinct, laths, which represent a major cumulus phase, and as fine-grained clusters, forming the interstitial material, which is a significant component of the sample. Grains are sub-euhedral to sub-anhedral and range from 0.5 - 4mm. Alteration has resulted in small patches of sericite flecks evolving throughout the thin section. Bent albite twins are caused by deformation. Magnetite is a minor cumulus phase and occurs as large angular grain, as small euhedral needles within pyroxene, and as vein infill. Their sizes range from 0.5 - 3mm. Pyroxene, a minor cumulus mineral, is mainly represented by clinopyroxene, and as inverted pigeonite in a minor role. Grains are 1 - 3mm and have a sub-anhedral appearance. Chlorite is absent. Biotite with grains measuring < 0.1 - 1mm, occurs at pyroxene margins and in association with magnetite, although occasional small, exsolved blebs can be seen within pyroxene grains.

234m (D2.211)
A high proportion of plagioclase occurs as fine-grained clusters forming the interstitial component. Most grains are fragments of originally elongate laths and these represent the major cumulus phase. Grain size is < 0.1 - 3mm and the shape is sub-euhedral to sub-anhedral. Alteration is absent. Deformation is prevalent in many plagioclase grains. Magnetite appears in two forms. Large angular grains appear both as a minor cumulus phase and as a component of interstitial material, whereas small exsolution needles are incorporated within pyroxenes. Both are between < 0.1 - 4mm in size. Pyroxene is a minor cumulus phase represented by clinopyroxene and inverted pigeonite, with grain sizes of 1 - 3mm and 0.5 - 3mm respectively. The latter exhibits several sets of exsolution lamellae, some showing signs of deformation. Alteration to chlorite is absent. Biotite occurs alongside magnetite as acicular grains and blebs up to 0.3mm in size. Quartz occurs in conjunction with the interstitial plagioclase.

202m (D2.243)
Plagioclase forms the major cumulus phase and part of the interstitial groundmass. Grains are sub-euhedral to sub-anhedral and are < 0.1 - 4mm in size. Grain edges display zonation and a high proportion of grain boundaries also appear fractured. Alteration is absent at this depth. Magnetite fulfils a minor cumulus role with a grain size of 0.1 - 4mm. It is present either as rounded blebs or as smaller euhedral exsolution needles, which are aligned sub-parallel to each other within pyroxene grains. Pyroxene is a minor cumulus phase with clinopyroxene the dominant mineral. Only minor amounts of inverted pigeonite are present. Grains are sub-anhedral and measure 1 - 2mm and 1 - 3mm, respectively. Alteration to chlorite has not occurred. Biotite grains, < 0.5mm in size, are found within the pyroxenes, often in association with magnetite.

163m (D2.282)
Plagioclase is present solely as a major cumulus phase. Grains are sub-euhedral to sub-anhedral and range from 1 - 5mm. Zonation is evident around grain edges. Alteration and deformation are absent. Magnetite is a minor cumulus phase and appears as < 0.1 - 5mm needles and blebs. The euhedral needles are observed as within pyroxene as exsolution lamellae, whereas the larger rounded blebs are scattered throughout the matrix. Pyroxene is present as a minor cumulus phase. Both clinopyroxene and inverted

pigeonite grains are 1 - 2mm, but the latter exists also as mottles measuring 5mm. Grain edges are visibly altered to chlorite. A few grains of biotite, measuring < 0.1mm, are observed at the grain boundaries of both pyroxene and magnetite.

111m (D2.334)
Clusters of fine-grained plagioclase form a small part of the interstitial groundmass, as well as retaining a major cumulus role. Grain size is 0.1 - 3mm. Alteration is visible as small needles invading the larger grains, which also display deformation in the form of bent albite twins. Magnetite occurs both as needles, as exsolution lamellae within pyroxene and as an interstitial component where blebs form at the boundaries of small-grained pyroxene clusters. The size ranges from 0.1 - 4mm. Pyroxene has a minor cumulus role. The largest component is clinopyroxene with grains measuring 1 - 2mm in size. Inverted pigeonite is also present with grains of 1 - 3mm. Minor alteration to chlorite is evident at grain boundaries. Biotite blebs of < 0.1mm occur in association with magnetite.

105m (D2.340)
Plagioclase is the major cumulus mineral. A small amount also occurs as interstitial material. Grains are mainly sub-euhedral to sub-anhedral and are 0.1 - 3mm in size. The mineral is generally fresh in appearance, although some blocky grains are fragmented. Deformation is absent. Magnetite, as an exsolution product, occurs as small euhedral needles within pyroxene. It also appears as interstitial rounded blebs or angular grains. Both forms have a size range of 0.1 - 1mm. Pyroxene is an intercumulus phase with clinopyroxene dominant over inverted pigeonite. Both minerals have grains between 1 - 3mm with fractured boundaries, which also show evidence of minor alteration to chlorite. Biotite, measuring < 0.1mm, is also apparent at pyroxene grain boundaries, but in negligible amounts.

89m (D2.356)
Plagioclase is present solely as the major cumulus phase, with sub-euhedral to sub-anhedral grains measuring 2-4m. Alignment along the length of the slide is clearly exhibited by elongate laths. Alteration, with consequent minor sericitisation, along fractures is visible within the majority of grains. The plagioclase laths also display very slight deformation. Magnetite is a minor cumulus phase represented by fine-grained blebs, which measure 0.1-2mm and are associated with the pyroxene component. Pyroxene is a minor cumulus phase composed of clinopyroxene and inverted pigeonite. Clinopyroxene grains are 1-2mm, whereas inverted pigeonite forms large, optically continuous mottles up to 5mm in diameter. Generally, the grains are partially altered to chlorite. Biotite is absent.

62m (D2.383)
Plagioclase occurs only as the major cumulus phase and consists of broken fragments and elongate laths ranging from 2-6mm. Alteration exists in patches where sericite has invaded. Albite twins exhibit minor deformation. Zonation is apparent in several grains. Magnetite is a minor cumulus phase, occurring in the interstitial areas and within fractures of the larger pyroxene grains. Both euhedral needles and small rounded blebs are noted and these range from <0.01-3mm. Intercumulus pyroxene is represented by clinopyroxene and inverted pigeonite in lesser amounts. Grains are 0.5-1mm and 1-4mm respectively. A sub-ophitic texture between the pyroxenes and the plagioclase grains is evident. Chlorite alteration is apparent at both grain boundaries and along fractures. Biotite, of <1mm, is found associated with magnetite. Secondary hornblende is also observed and ranges from 2-3mm.

46m (D2.399)
Plagioclase only occurs as the major cumulus phase. Many of the sub-euhedral to sub-anhedral grains, which range from 2 - 5mm, have a distinct myrmekitic texture. Alteration to sericite is minor and there is little evidence of deformation of the plagioclase. Magnetite is present only in the interstitial groundmass,

represented by small euhedral needles and blebs, which measure 0.1 - 4mm. Pyroxene is an intercumulus phase with both clinopyroxene and inverted pigeonite occurring. Grains are 1 - 3mm and 1 - 4mm respectively and exhibit a sub-ophitic texture with the plagioclase. Minor alteration to chlorite is evident as small patches within grains and also at grain boundaries. Biotite is absent.

37m (D2.408)
Plagioclase is present only as the major cumulus mineral. Myrmekitic textures are clearly noticeable within many of the grains, which are 1 - 4mm. Numerous grains are elongate and fragmentation is conspicuous. Very small patches of alteration occur throughout. Magnetite appears only in an interstitial role as rounded blebs of 1 - 4mm between plagioclase and pyroxene. Pyroxene is an intercumulus phase with clinopyroxene dominant over inverted pigeonite. Both minerals exhibit a sub-ophitic texture where incorporation of plagioclase has occurred. Grain size is 1 - 3mm and 1 - 4mm respectively with optical continuity retained over large areas. Small quantities of chlorite exist at grain boundaries where minor alteration has taken place. Biotite is absent.

14m (D2.431)
Plagioclase is the major cumulus mineral. Myrmekitic textures are found at the edges of the larger grains, which measure 3 - 8mm. A sub-ophitic texture is apparent in the smaller grains, which are incorporated within the pyroxenes. These are 0.5 - 1mm in size and are more euhedral in shape. Slight deformation has resulted in bent albite twins. Magnetite, present as small euhedral exsolution needles of < 0.3mm within the pyroxenes. As an interstitial mineral, it occurs at the boundaries of the larger plagioclase and pyroxene grains. Pyroxene is an intercumulus phase, with both clinopyroxene and inverted pigeonite occurring as large mottles that retain optical continuity up to 10mm and 7mm respectively. Alteration to chlorite is noted at grain boundaries. One grain shows secondary hornblende replacement. Biotite occurs as tiny acicular grains of < 0.1mm in association with magnetite.

4m (D2.441)
Plagioclase is present only as the major cumulus phase. Grains are sub-euhedral to sub-anhedral and are 1 - 5mm. Alteration to sericite has occurred in minor amounts and zonation is evident in only a few grains. Deformation has resulted in bent albite twins, but these are ill-defined. Magnetite is a minor cumulus phase. It exists as very small euhedral exsolution needles of < 1mm within pyroxene grains. Pyroxene is an intercumulus phase, with both clinopyroxene and inverted pigeonite exhibiting an ophitic texture with plagioclase. Grains are 1 - 4mm and 1 - 3mm respectively and have a sub-euhedral appearance. Alteration to chlorite is minor and found mainly at grain boundaries. Biotite occurs as blebs up to 1mm in association with magnetite.

-3m (D2.448)
Plagioclase only occurs as a major cumulus phase. Grains are 1 - 5mm and exhibit diagonal alignment across the thin section. The majority are small and blocky, with only a few elongate laths present. Alteration, deformation and zonation are not evident. Magnetite is absent. Pyroxene is an intercumulus phase and is represented mainly by clinopyroxene, which has a grain size of 1 - 4mm. Minor amounts of primary orthopyroxene, measuring 1 - 6mm, are present. Both minerals are sub-anhedral and exhibit a sub-ophitic texture with plagioclase. Inverted pigeonite is absent. Alteration to chlorite is minor and occurs at grain edges. Biotite measures < 0.5mm.

-22m (D2.467)
Plagioclase occurs as the major cumulus phase. Grains are sub-euhedral to sub-anhedral and are 1 - 3mm in size. Small patches of alteration to sericite occur throughout the sample. Deformation has caused albite twins, which are ill-defined, to bend. Magnetite is found as tiny intercumulus needles, which are <